AN ANALYSES of ISSUES REGARDING the INTERPRETATION of VLF DATA Utilizing PLANE WAVE TECHNIQUES

In recent years, there has been a trend to place VLF equipment on low flying vehicles such as drones and helicopter stingers. Survey companies offering such services also offer or suggest the interpretation of such data with software using plane wave sources. Such software is otherwise used to model and invert magnetotelluric data.

The VLF field is generated by man-made 3D antennae but principally groups of antennae. While in most instances, it is assumed that the data will be collected in the far field, we ask the question whether VLF data can be properly interpreted as due to a uniform, plane wave propagating downwards..

From our analyses and conclusions, we believe that VLF data cannot be interpreted with MT software without careful human analyses and any plane wave tipper inversion cannot provide correct results.

To represent VLF fields, two issues must be included in the simulation capabilities. First, a line antennae in the air which is <u>not</u> grounded and second full wave propagation must be included. That is, a quasi-static approximation to the simulation code is not adequate.

This study was initiated as a result of attempt to interpret VLF data collected via antennae mounted on a helicopter stinger.

June, 2024 RW. Groom Eikon Technologies Ltd

CONVENTIONS

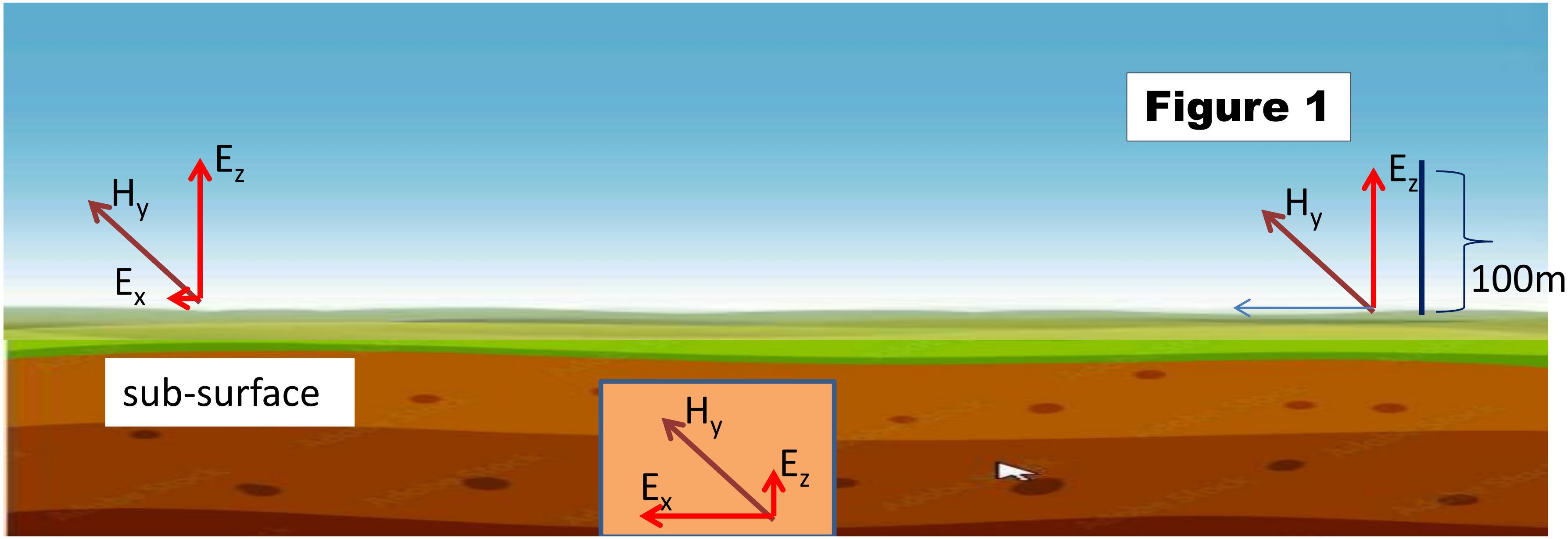

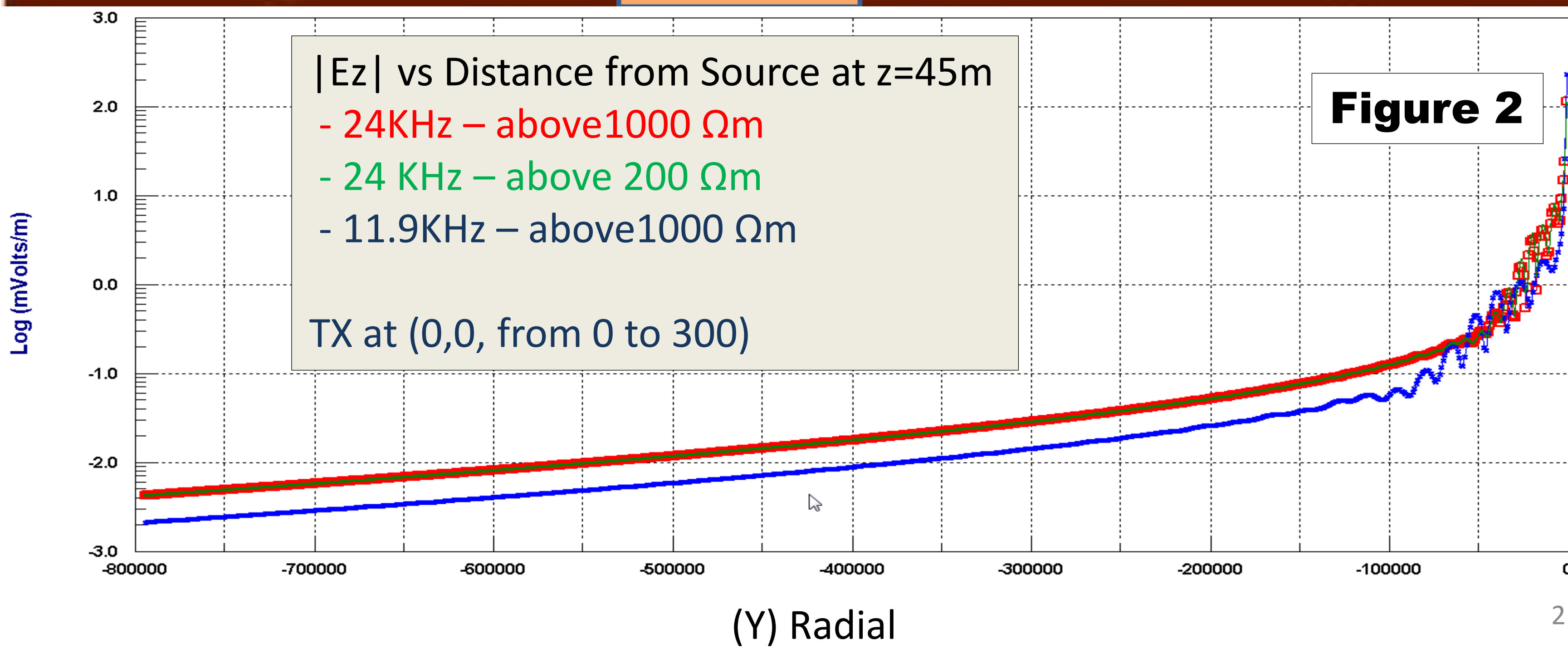

CONVENTIONS

In the figure below repeated from the previous page (Fig2), we plot the amplitude of the vertical electric field (Ez) as the field above ground at as it radiates from the vertical ungrounded source having a length of 100m positioned at (x=0,y=0). In this case, we have plotted |Ez| versus the y-coordinate travelling south. The choice of the direction of the data was simply because our survey data was south of the transmitters at Seattle and Cutler. The direction of propagation could have been in any radial direction from the source. Ez is the total response, direct wave plus ground scattered.

We have shown the results for 2 frequencies (24 and 11.9 Khz) and for 2 halfspaces with different resistivities. Within 50 to 100m from the source, the oscillating propagation produces relatively short wavelength oscillations in the amplitude. Beyond 100m, the oscillations are not noticeable in the amplitude of Ez and the field falls off a r^{-2}. The resistivity of the air was taken to be 10^8 Ωm. The amplitude in air never becomes 1/r.

On the next page, Figs 3&4, we zoom in on a smaller subset of the data and show the sinusoidal oscillations of the real and imaginary parts of Ez for 24Khz over 1000 Ωm. The wavelength (λ) here is 12.49 km, little changed from an infinitely resistive media. The phase shift between real and imaginary peaks and troughs is approximately 7km.

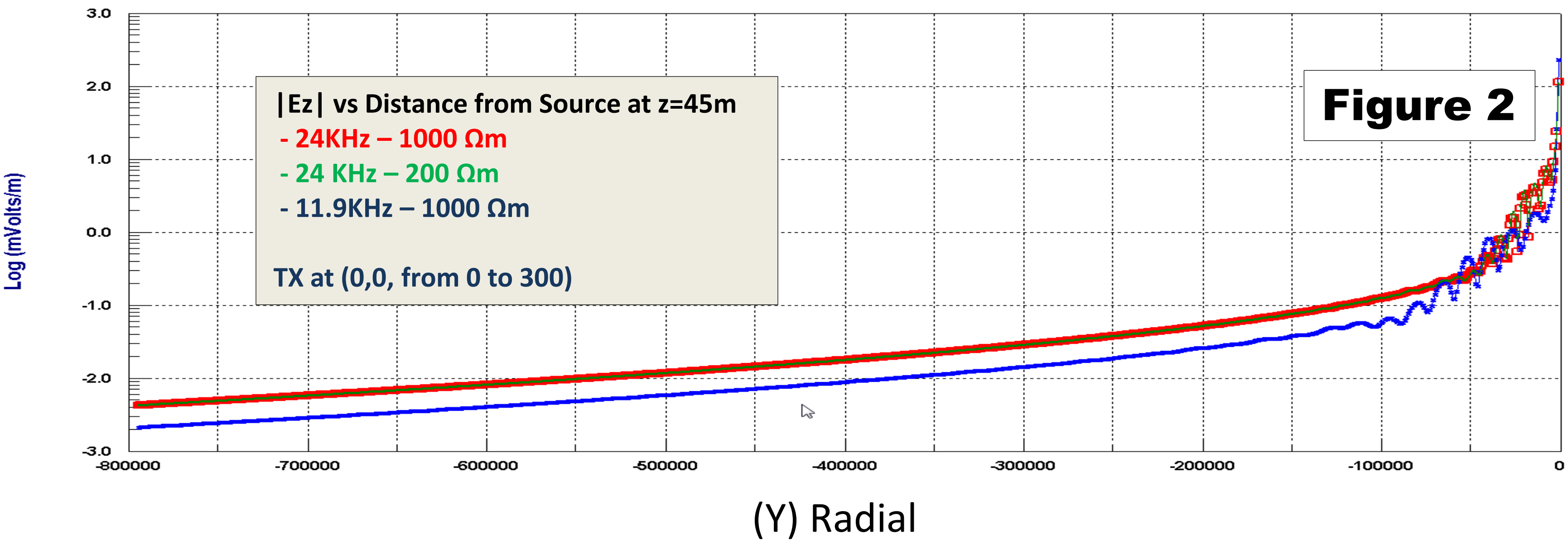

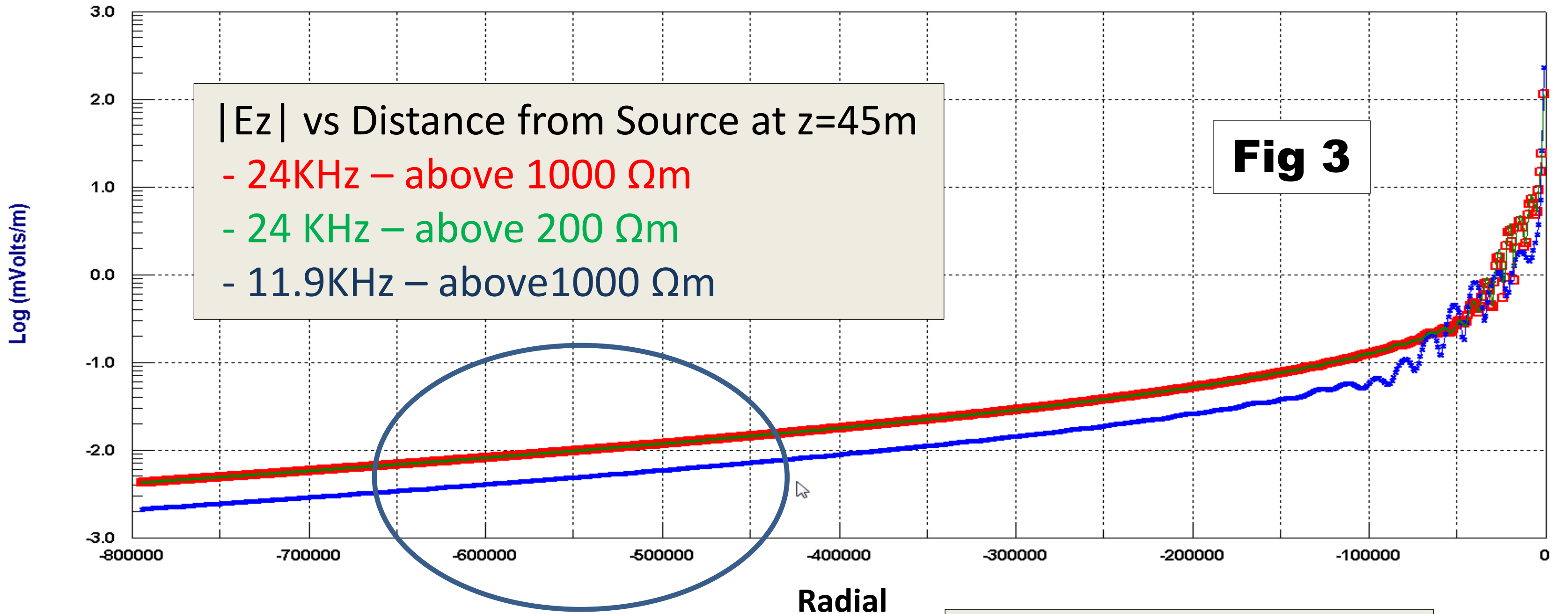

|Ez| vs Distance from Source at z=45m
- 24KHz – above 1000 Ωm
- 24 KHz – above 200 Ωm
- 11.9KHz – above1000 Ωm
Fig 3
Log (mVolts/m)
3.0
2.0
1.0
0.0
-1.0
-2.0
-3.0
-800000
-700000
-600000
-500000
-400000
-300000
-200000
-100000
0
Radial

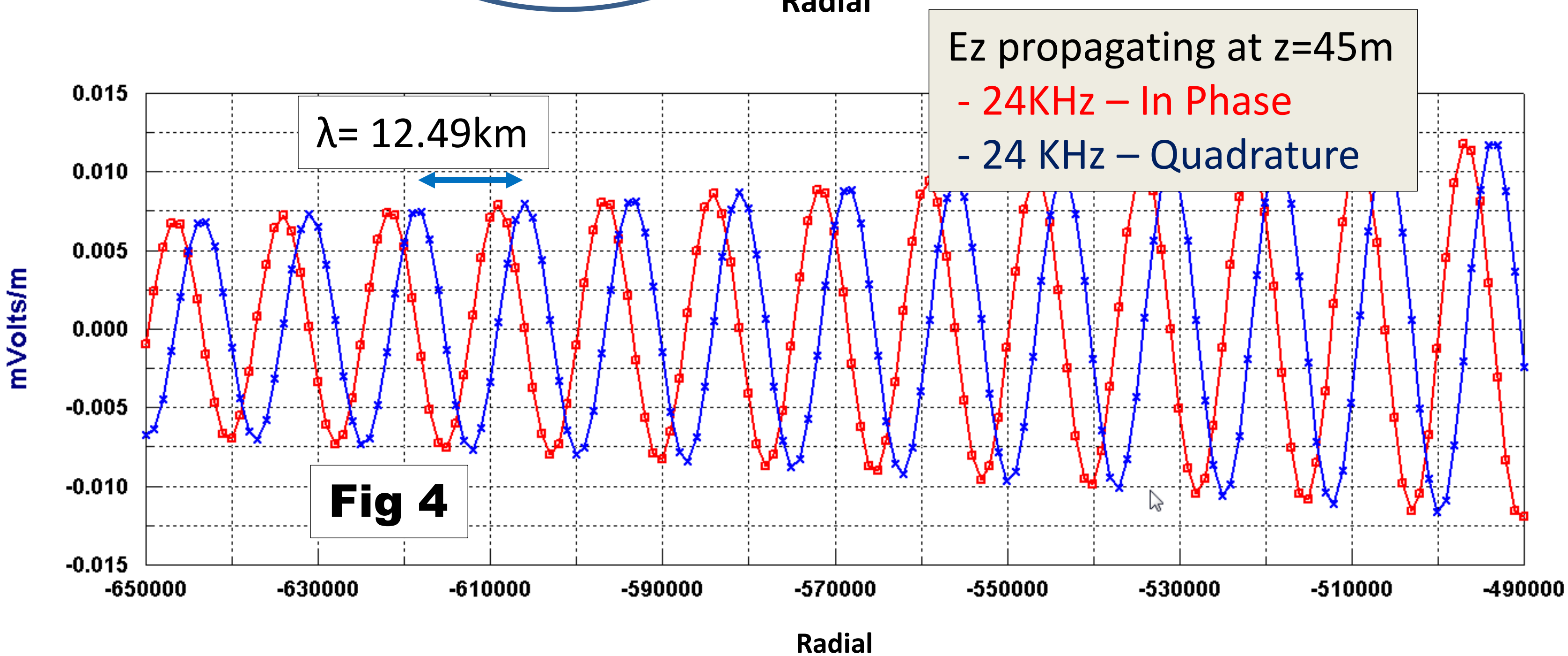

Ez propagating at z=45m
- 24KHz – In Phase
- 24 KHz – Quadrature
λ= 12.49km
Fig 4
mVolts/m
0.015
0.010
0.005
0.000
-0.005
-0.010
-0.015
-650000
-630000
-610000
-590000
-570000
-550000
-530000
-510000
-490000
Radial

VLF Simulation

- The VLF antennae is simulated in all examples as a vertical ungrounded line antennae with a 1000 Amp current.
- In most instances, the real world VLF antennae consists of a number of vertical antennae with a mesh of wiring above (umbrella) and below creating a capacitor to enhance the signal. Due to the accuracy of the algorithms and lack of any noise, we do not need this enhancement.
- As examples, the Cutler and Seattle antennae are more than 300m in height.
- In most examples, the atmosphere is simulated as a resistor at 10^8 Ωm and the ground at varying halfspace or layered resistivities.
- The simulation is essentially analytic requiring only the fulfillment of boundary conditions at the horizontal interfaces and a straightforward but accurate Hankel transform.

Vector Conventions

- The X,Y components are horizontal. In most models, the X component is the azimuthal direction to the antenna source (Figure 1). The Z component is normal to a flat earth in all simulations.

VLF Fall Off and Propagation

- At shallow elevations above ground, propagation is primarily in a horizontal direction and independent of azimuth.
- Primary radiation fields are E_z and the horizontal component, H_y. Both fields are perpendicular to the direction of propagation
- In the air, fall-off is primarily geometric at a rate of r^{-2} except near the antennae (Figure 2)
- The wavelength in the air is approximately 12km at 25Khz with a skindepth of 530km (Figure 4). [$\rho=10^8$, $\varepsilon_r = 1$]
- In the earth just below ground level, the wavelength in 1000 Ωm (for example) is 632m with a skindepth of 100m.
- There is a slight rotation of E (Fig5) in the air towards the horizontal when a strongly conducting ionosphere is not present. Otherwise there is no rotation.
- Below the earth's surface, the electric field becomes almost entirely horizontal (Figure 6) directed in the direction of propagation in a layered earth.
- Ez still persists below the surface with its amplitude depending upon the resistivity of the ground. However, its effect is not considered essential to simulating the response of anomalies.
- Primary Ex (direct plus background) in the ground (next page) does decay with an overall r^{-1} .
- The horizontal electric field in the direction of propagation, Ex, still maintains a strong gradient along the direction of propagation as well as azimuthally (Figure 6). These factors may affect the accuracy of plane wave modeling depending upon the size of the anomalous structures. These issues are examined below.
- In the following figures, we see that the Ex field both in the air and on the surface over a halfspace or layered earth have the same spatial variation . This effect is simply because Ex is continuous across the earth's surface. The cyclical variation of Ex in the following example is 236km. There appears to be some interplay between the wavelength of the E field in the air and the skindepth in the ground (Figure 8). We have not fully investigated nor understood this issue.

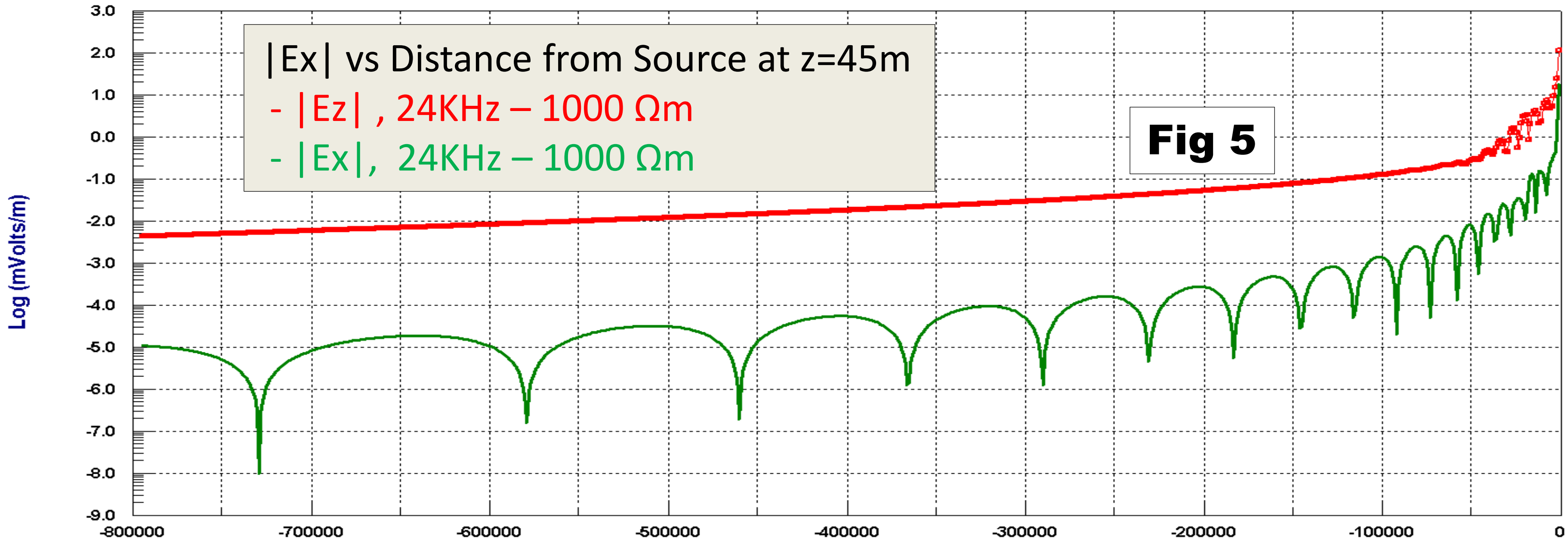
|Ex| vs Distance from Source at z=45m
- |Ez| , 24KHz – 1000 Ωm
- |Ex|, 24KHz – 1000 Ωm
Fig 5
Log (mVolts/m)
3.0
2.0
1.0
0.0
-1.0
-2.0
-3.0
-4.0
-5.0
-6.0
-7.0
-8.0
-9.0
-800000
-700000
-600000
-500000
-400000
-300000
-200000
-100000
0

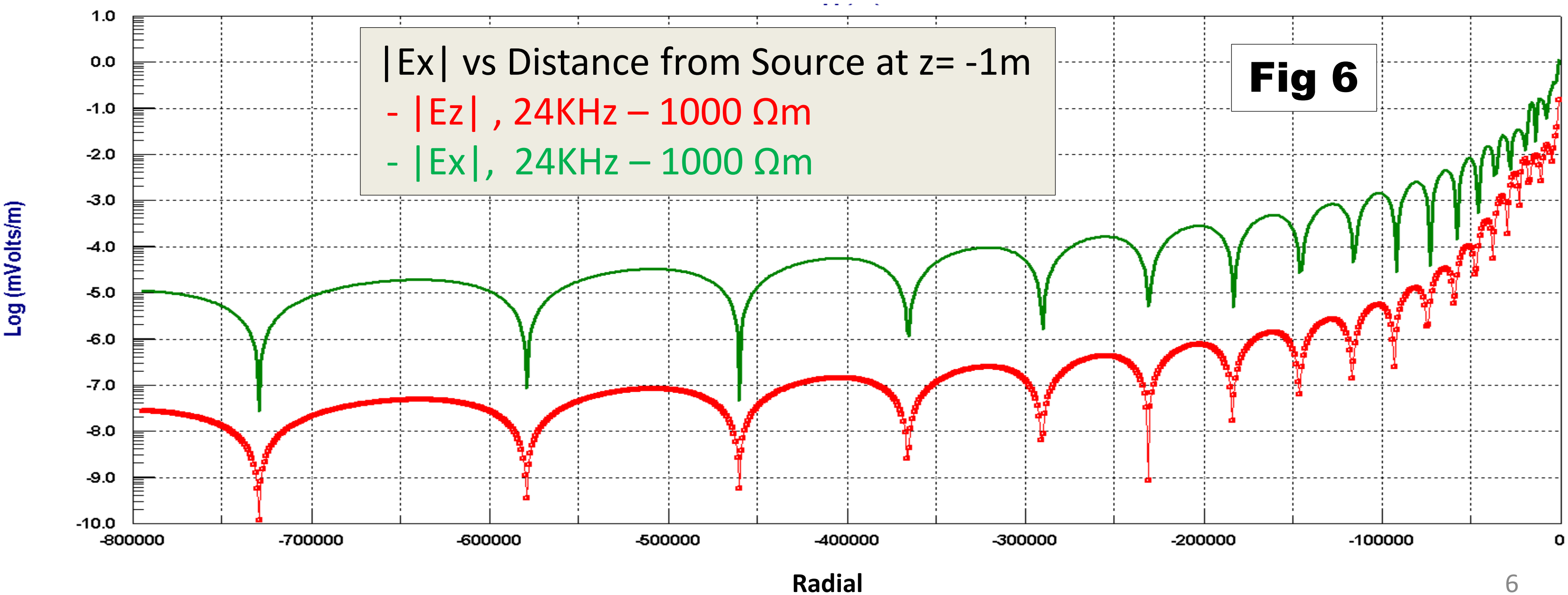
|Ex| vs Distance from Source at z= -1m
- |Ez| , 24KHz – 1000 Ωm
- |Ex|, 24KHz – 1000 Ωm
Fig 6
Log (mVolts/m)
1.0
0.0
-1.0
-2.0
-3.0
-4.0
-5.0
-6.0
-7.0
-8.0
-9.0
-10.0
-800000
-700000
-600000
-500000
-400000
-300000
-200000
-100000
0
Radial

Spatial Variation in the Principle Source Fields

In Figure 5, we plot, at a height of 45m above the ground over a distance of 800km, the amplitude of the vertical electric field (Ez) and the amplitude of the horizontal electric field component (Ex) in the azimuthal direction from the source. The azimuthal direction is the direction of propagation. The frequency is 24Khz and the ground resistivity is a halfspace of 1000Ωm. The fall-off of Ez at a distance from the source is r^{-2} but the oscillation in amplitude is not distinguishable at this scale (see Fig4). The oscillation in Ex, however, is easily seen. The transition from a minimum to a maximum increases with distance but the overall fall off in amplitude is also r^{-2}. |Ez| is over 200 times larger than |Ex|

For Figure 6, the fields and settings are the same except that now the fields are calculated at a depth of 1m below the air/ground interface. As these are quasi-analytic solutions, the accuracy at such a distance from the interface is not compromised. As expected, |Ex| does not vary much from its response at a height of 45m except close to the source. But, |Ez| is now over 200 times smaller than |Ex|. The spatial variation in |Ex| at z at -1m is unchanged from z at 45m except near the source. |Ez| can be seen to have the same spatial variation as |Ex|.

The spatial strong spatial variations in |Ex| over distances of order 100km are propagation effects combined with the response of the air/ground interface. These issues are examined in more detail on page 9 and 10.

VLF Impedances (Z)

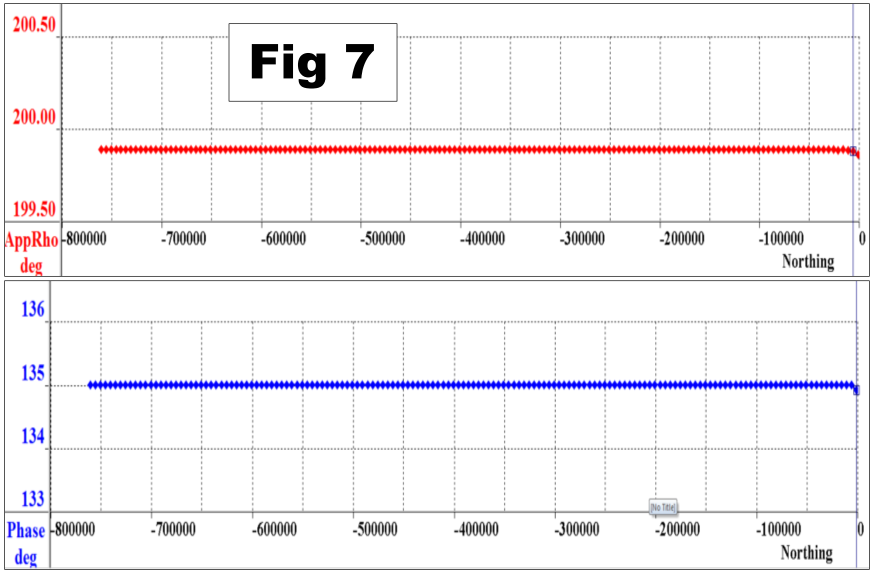

Despite the lateral propagation, the principal E and H fields of the VLF within the ground still approximately satisfy the MT apparent resistivity and phase relations at least for a halfspace and simple layered earth models. This we have determined by numerical experimentation. This confirms that the wavelength, skin depth and radial geometric fall-off of the principal E and H fields are the same and there ratio is controlled by the ground resistivity or impedance.

Z vs Distance at z= -1m
- ρ , 24KHz – 200 Ωm
- ϕ, 24KHz – 200 Ωm

With a 200 Ωm halfspace (Fig7), except near the source, the apparent resistivity is 199.9 Ωm and the phase is 135.02 degrees. In this example, the current in the transmitter flows up. Thus if down, the phase would be about 45 degrees as in MT.

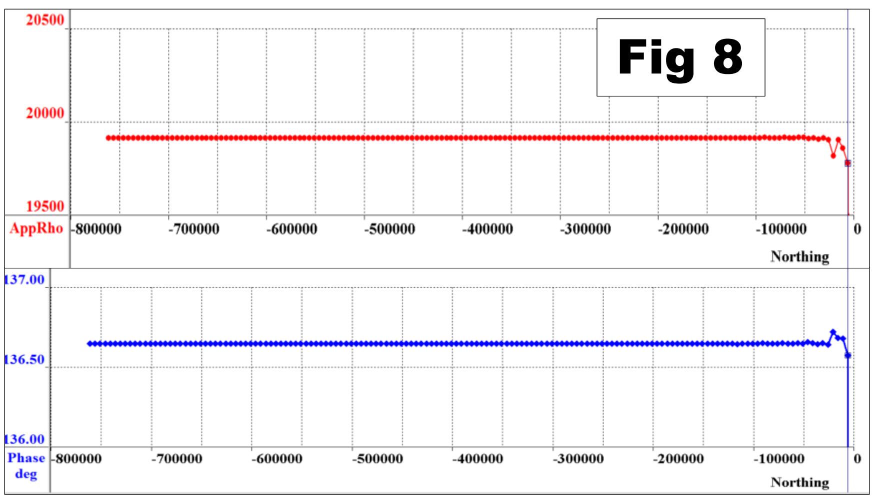

For a halfspace of 20K (Fig 8), starting at a distance of about 50km from the source, the apparent resistivity is 19916 Ωm and the phase is 136.6 degrees.

Z vs Distance at z= -1m
- ρ , 24KHz – 20000 Ωm
- ϕ, 24KHz – 20000 Ωm

Spatial Variation in the Principle Source Fields (cont'd)

In Figure 9, we follow up with a close up of the spatial variation over a distance of 400km starting at 400km from the source. Here, we plot only the inphase (real) part of Ex in order to see the nature of the variation. The frequency of the fields are unchanged from Figures 5 and 6 and the ground resistivity is unchanged.

The top figure below is the Re[Ex] at a height of 45m above the resistive ground and the bottom figure is the same field but at 5m below the ground. At this frequency (typical VLF frequency), there is little variation between the response in the air and that in the air. But, the peak to peak variation is 235km as compared to the wavelength of 12.49km of Ez in the air. Although, this is long wavelength effect, there is a constant gradient in Ex and two locations within each oscillation where the field changes sign.

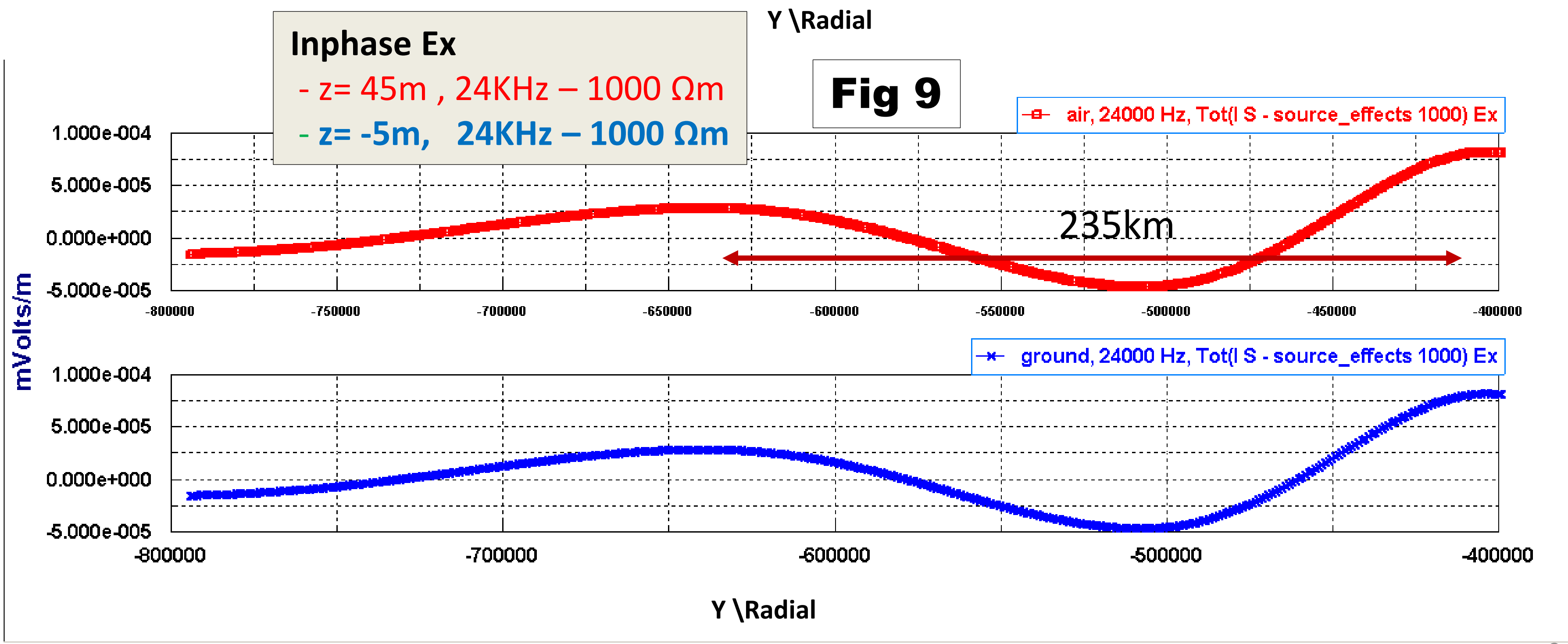

VLF Source Spatial Gradients:

- For modeling and inversion of magnetotelluric data, we must make assumptions in order to simulate models or perform inversion as the details of the source field are unknown. These assumptions include that there are no horizontal gradients in the source field about the structures of interest and the decay of the source field vertically is controlled by the skin depth.
- We will examine first the horizontal gradients of the VLF source field within the earth and then to determine if the vertical decay is solely due to the skin depth. Below (Figure 10), the main source fields Hy and Ex are shown at a depth of 45m. The southerly propagation is still seen in the fields below surface. This is to be expected as both these fields are continuous across the earth-surface boundary.

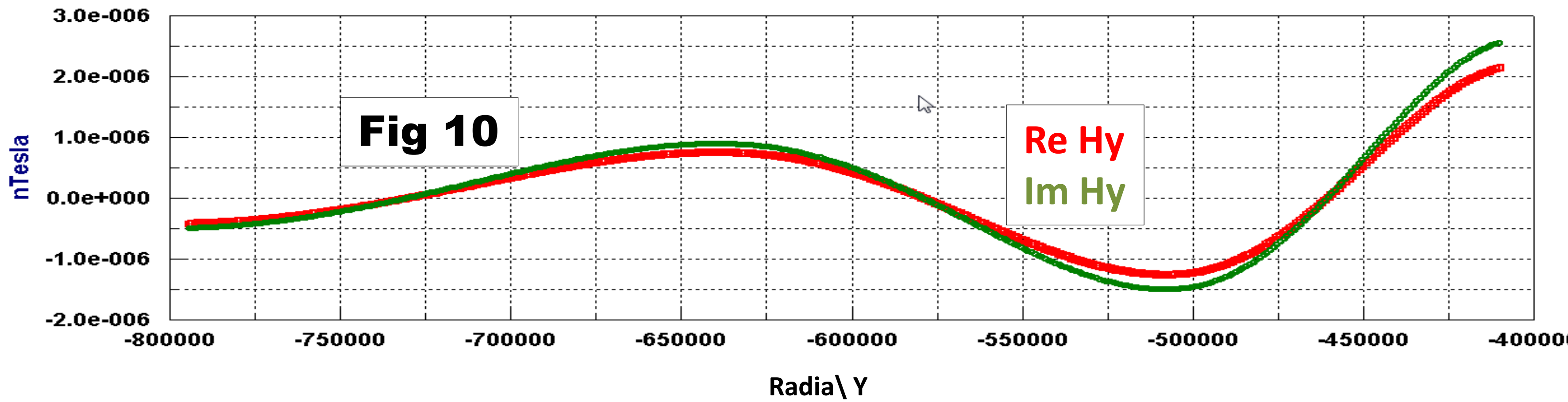

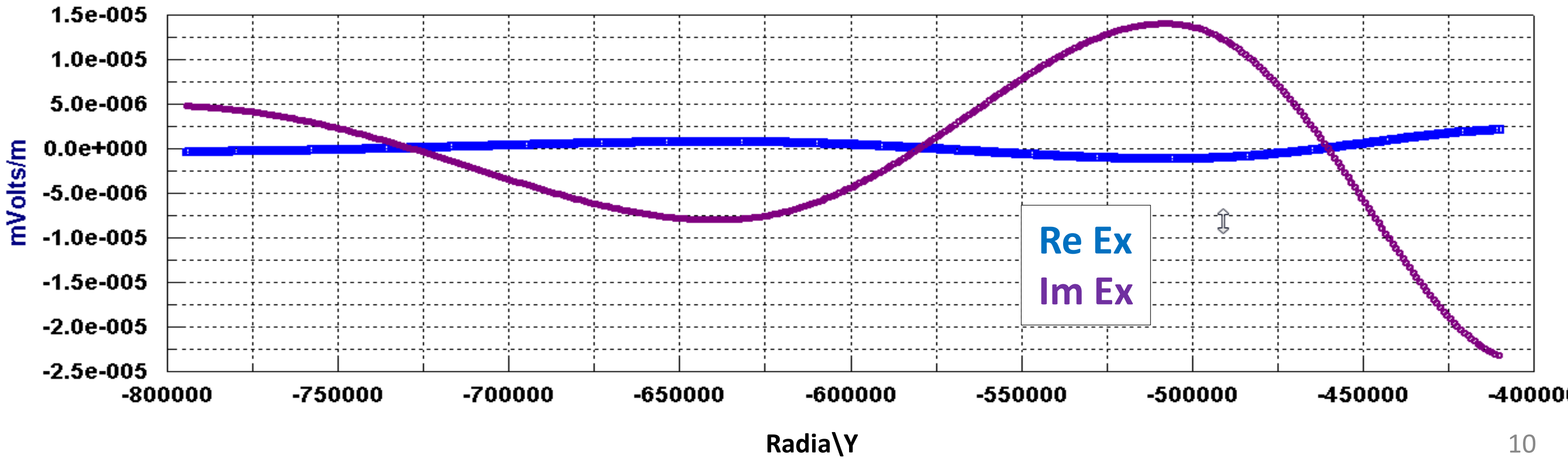

VLF Source Spatial Gradients:

- The VLF fields continue to propagate even as the distance from the source gets extremely far. The two main exciting fields from the VLF source are Hy perpendicular to direction of propagation and Ex parallel to the source polarization are horizontal. These fields are therefore continuous through the surface of the earth and the propagation is therefore still seen within the earth. Although, in many locations the horizontal gradients are not large, there are numerous locations (Figure 12) where this is not the case as seen below again at a depth of 45m.

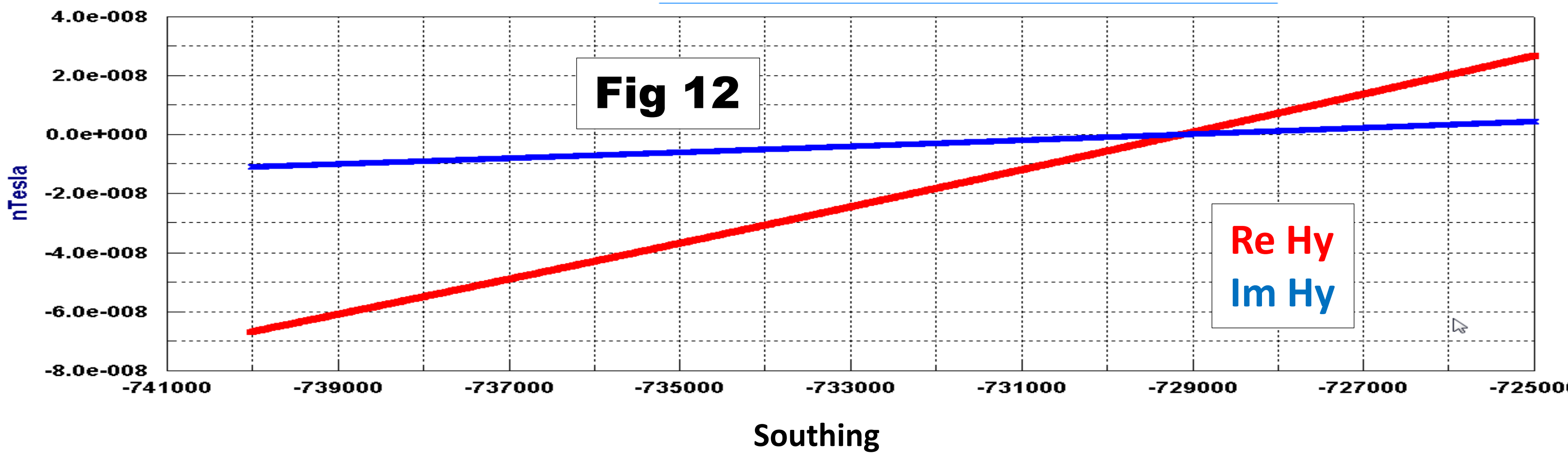

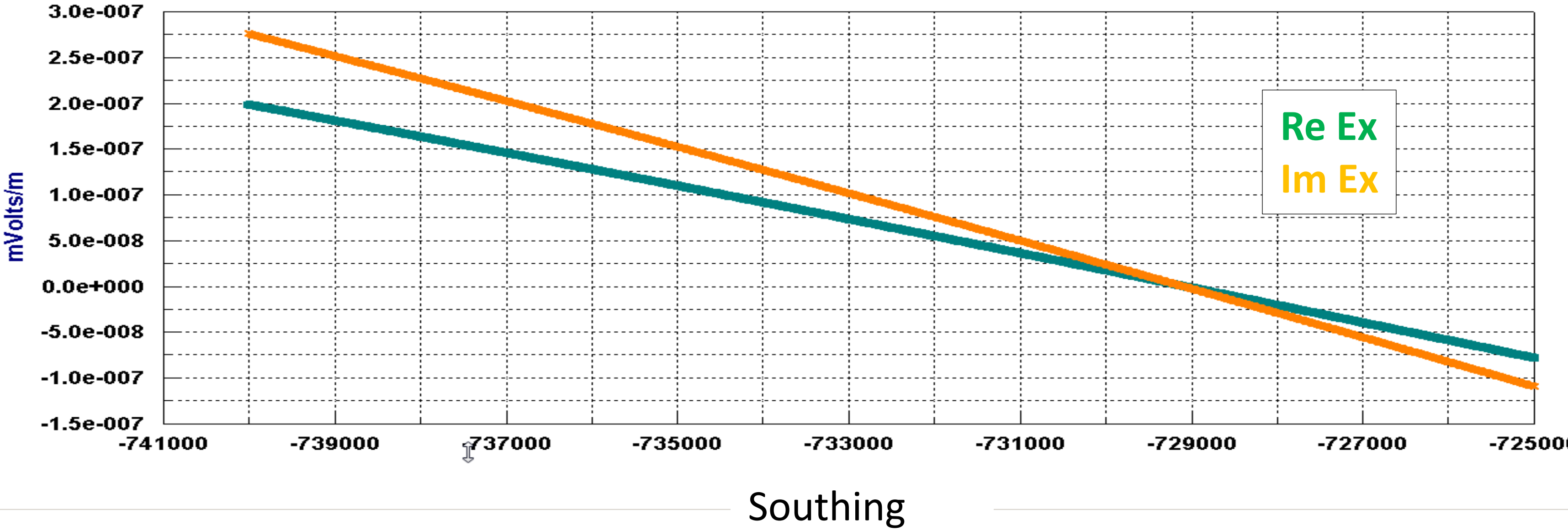

VLF Source Spatial Gradients:

- The VLF fields continue to propagate even as the distance from the source gets extremely far. The two main exciting fields from the VLF source are Hy perpendicular to direction of propagation and Ex parallel to the source polarization both are horizontal components.

- Below, is shown the phase of the primary Ex within the earth at a depth of 45m. The effects of the lateral propagation and the resistivity contrast at the earth's surface causes changes in the direction of this primary exciting field. The same is true for the primary magnetic field, Hy. This is completely contrary to our assumptions when modeling MT data which utilizes a uniform, plane wave source field.

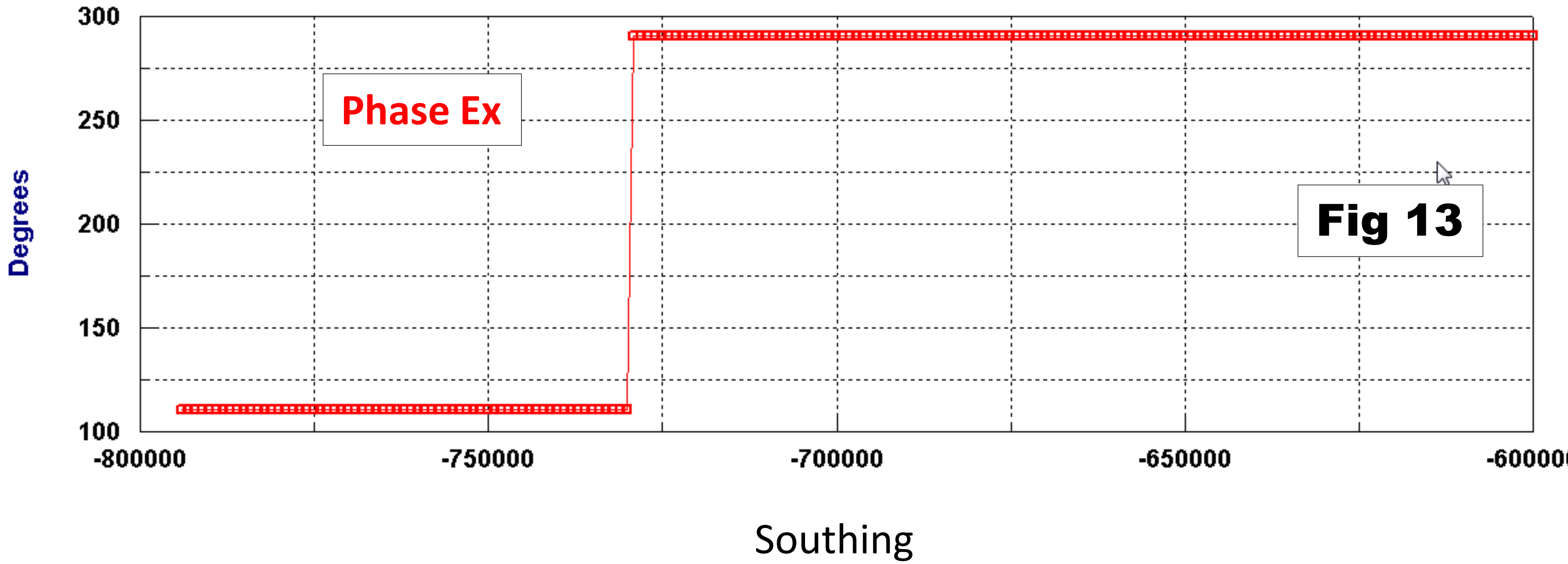

Fig 13

VLF Source Spatial Gradients:

- Next, is the question of the lateral variations in the VLF source fields perpendicular to a profile directed away from the source. Gradients of the source fields perpendicular to a radial survey line are very small. There is now a perpendicular source field, Ey, but it is very small compared to the principal current source. Results are similar for the Hx source fields. In general, these results would allow MT interpretation approaches.

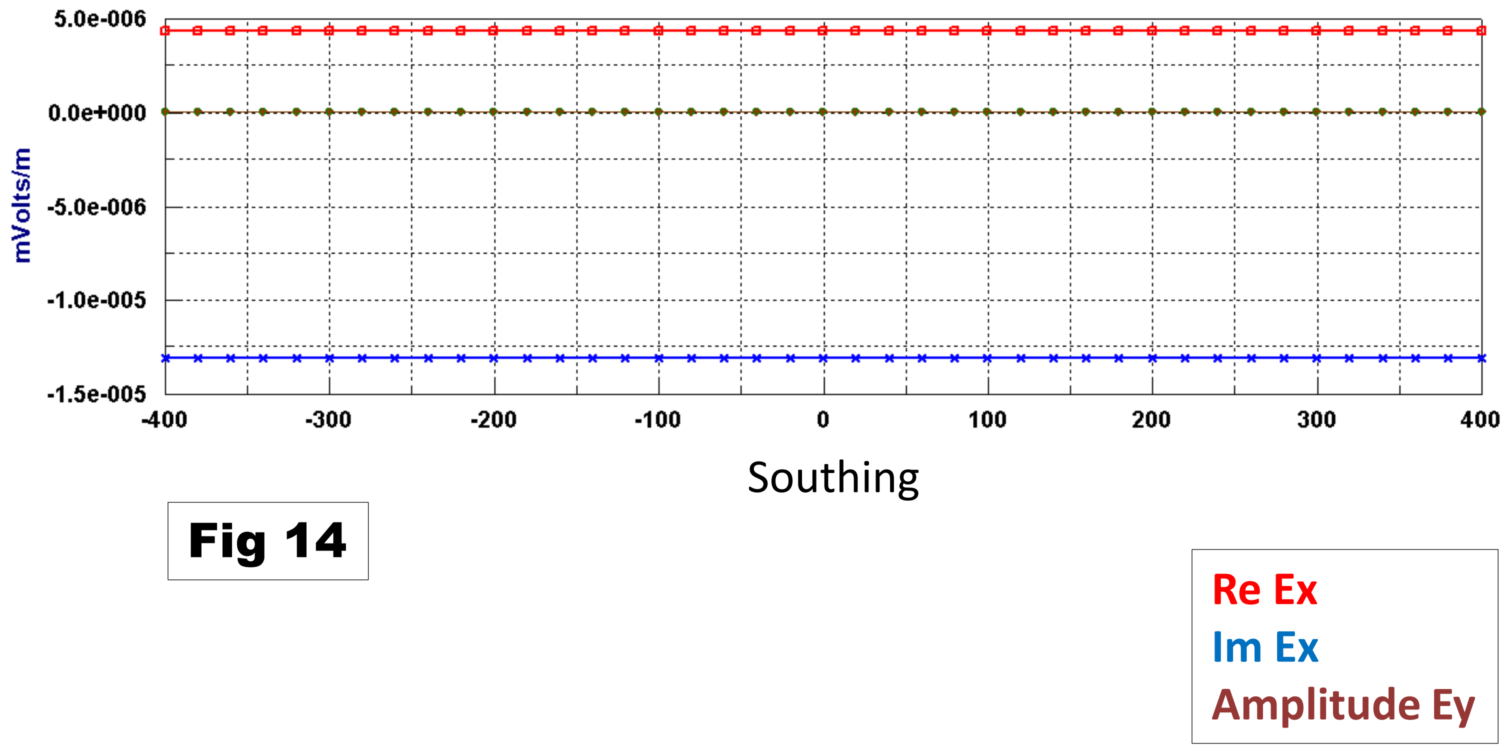

Fig 14

VLF Source Vertical Gradients:

- The VLF source fields have both a geometric falloff as well as sinusoidal variations due to propagation. But, do these variations affect the fall-off of the fields vertically as compared to the MT source fields. The MT source fields are, of course, assumed to be horizontally constant but decay with skin depth vertically.

- The amplitudes of the VLF source fields and MT fields cannot be directly compared as they are simulated assuming different source strengths. We thus normalize the MT data to have the amplitudes of the respective VLF fields at the surface.

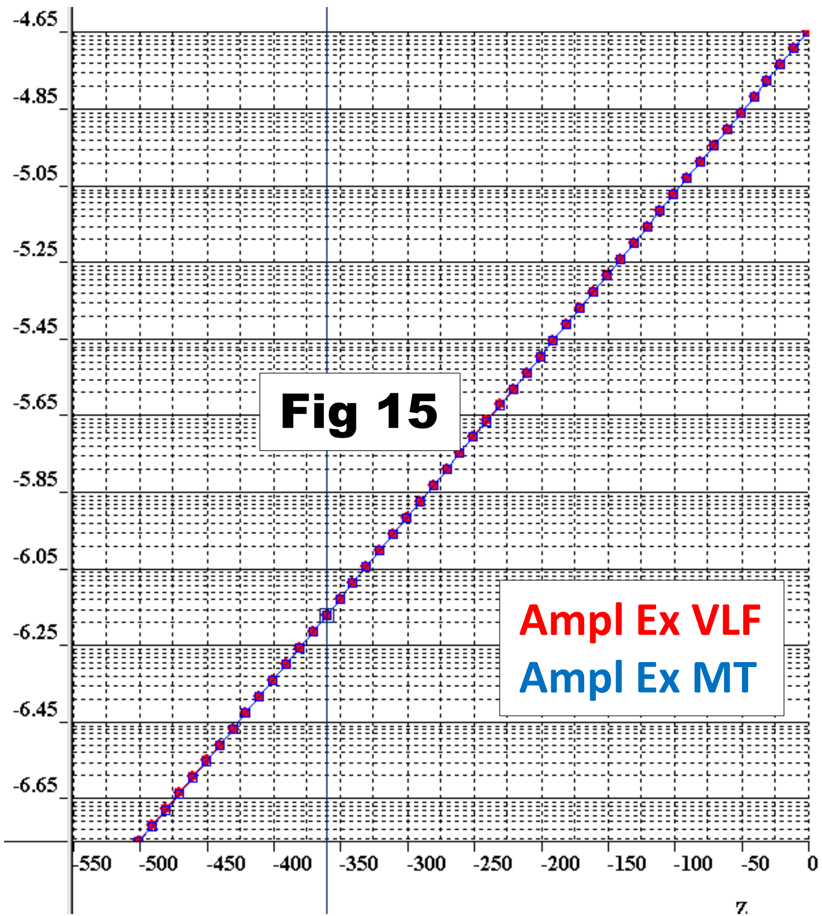

Depth

- The figure to the left is the horizontal primary electric field, Ex, amplitude compared for VLF and MT. The MT has been normalized to have the same amplitude as the VLF as the surface location.

- There are some very slight differences but not significant to interpretation. Results for the primary horizontal magnetic field are similar.

VLF Source Vertical Gradients:

- While the decay of the VLF source fields in the conducting host is controlled by the skin depth of the media, the amplitude is affected by the lateral distance along the propagation direction. In this case, the three stations are separated by 40Km. The example, Figure16, is for a 1000 Ωm halfspace.

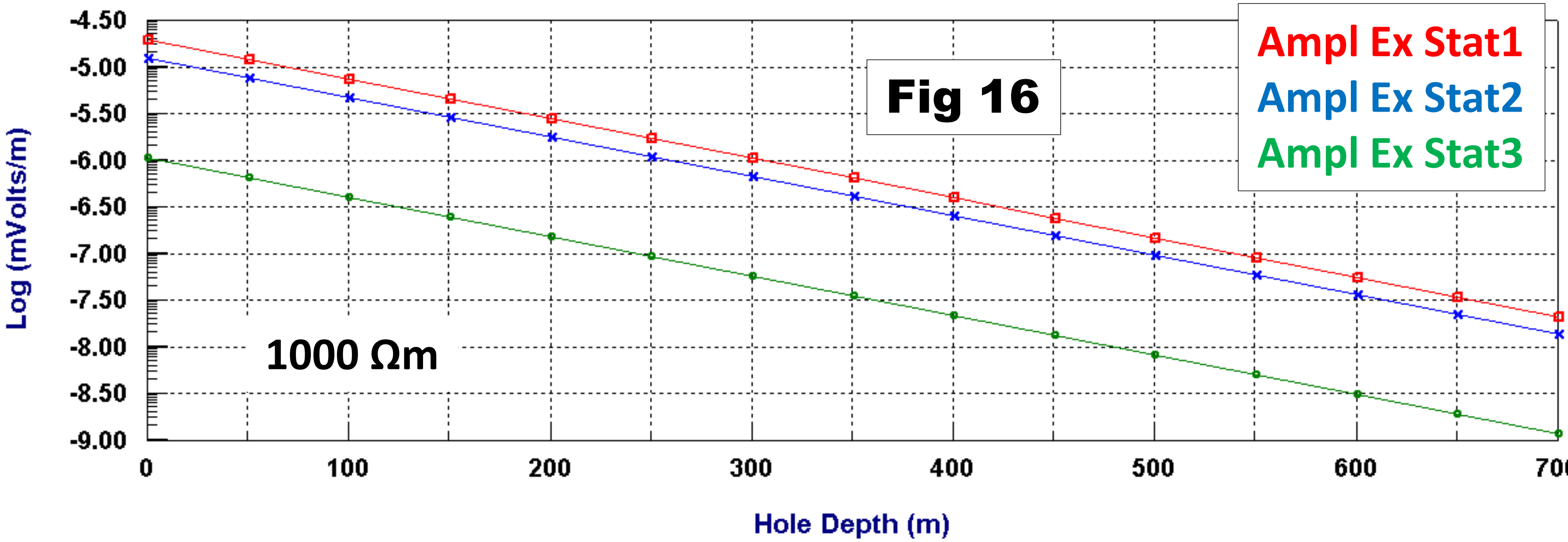

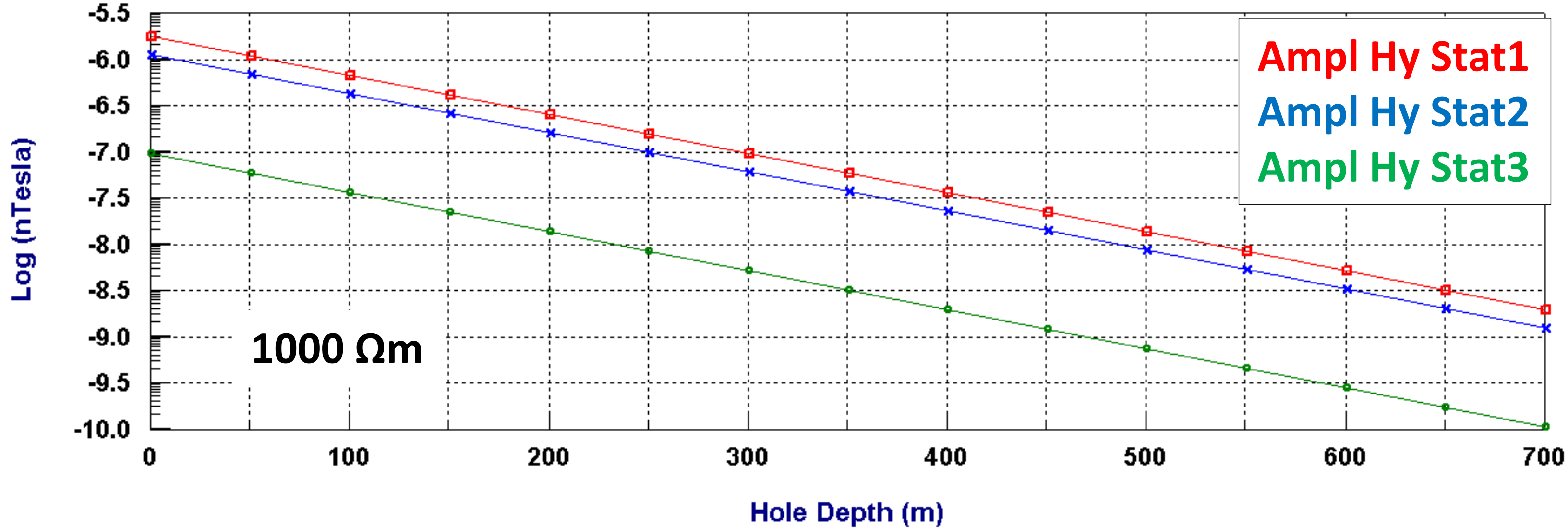

VLF Source Vertical Gradients:

- As Ez is the principle propagating component from the antennae through the air, there still persists an Ez below the surface. **J** normal is continuous and thus the amount of Ez in the ground depends upon the moisture in the air and the resistivity of the subsurface. Below, are the results for a highly resistive air and a subsurface of 100,000 Ωm. The air is 10^{*8} Ωm. The ratio of E_x/E_z is approximately 20.

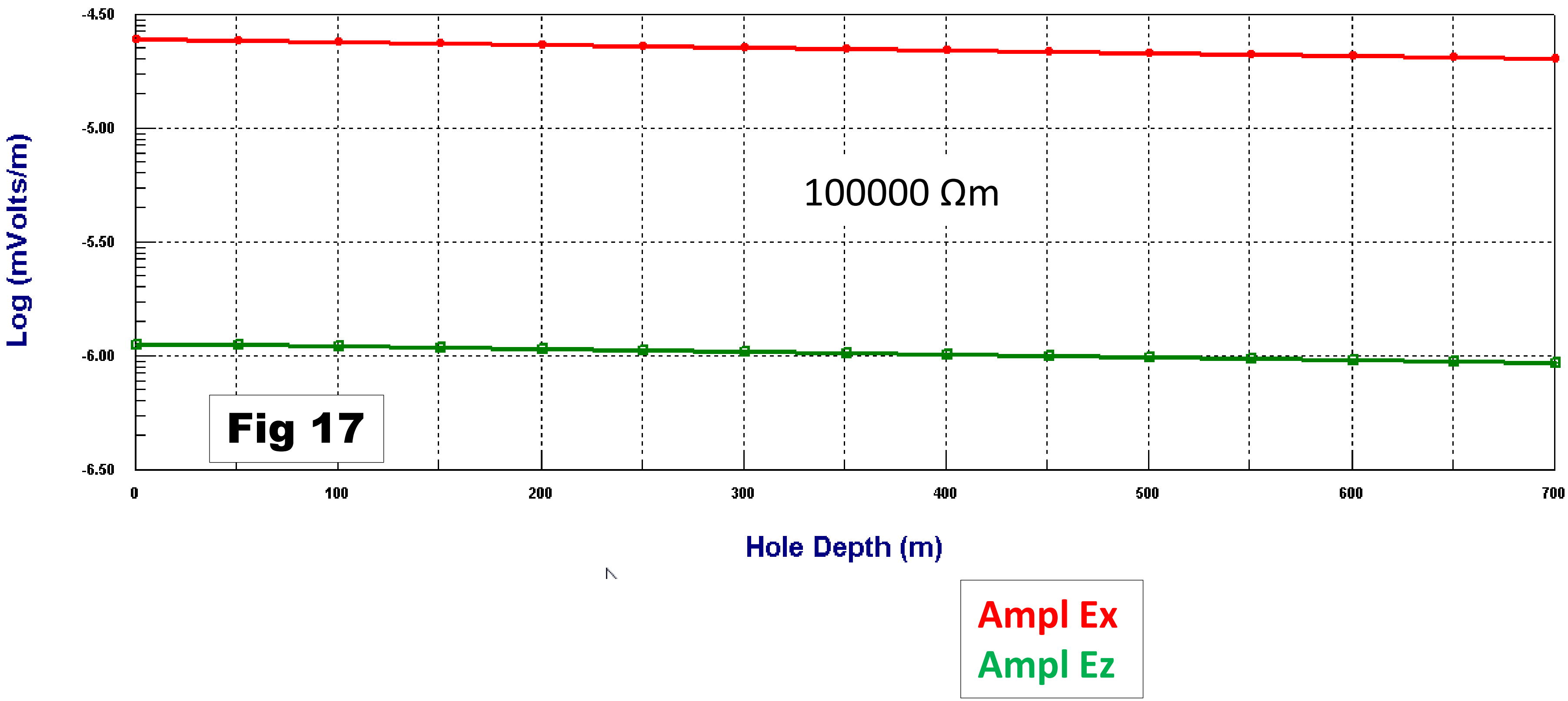

Fig 17

Types of Anomalies Studied:

For such a source field, it is reasonable to consider the TE response of anomalies.
TE (transverse electric) anomalies are parallel to the polarization of the horizontal electric field
In this case, we have a 2D source (azimuth independent) and 3D structures, the TE response is not necessarily equivalent to these modes in Magnetotellurics but rather to standard engineering definitions

- *Anomaly 1: parallel to direction of propagation and to the principal horizontal electric field within the ground. Weak conductor to imitate fracture or fault. The structure causes an anomalous current parallel to the Ex source field and thus causing a magnetic field to rotate about the anomalous current*
- *Anomaly 2: parallel to direction of propagation and well coupled to horizontal magnetic field within the ground. A strong conductor to represent, for example, a metallic structure. The source Hy fluxes through the conductor inducing current circulating inside the structure about the incident magnetic field*
- *Anomaly 3: resistor perpendicular to the main current source, Ex .*

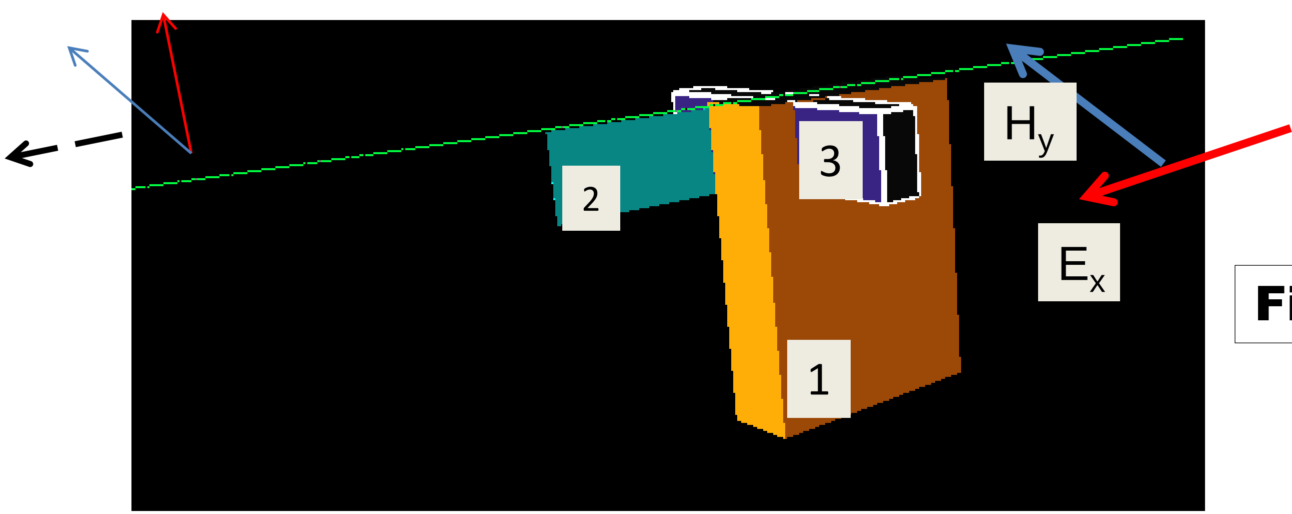

Fig 18

Types of Anomalies:

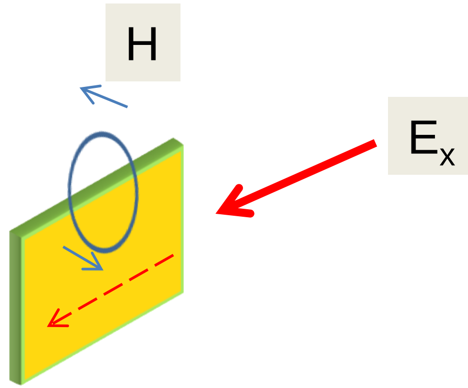

Channelling Anomaly
- Continuity of **J** normal creates an anomalous current within the conductor.

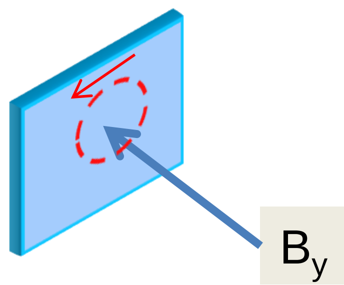

Inductive Anomaly
- flux of B through the anomaly creating currents (Faraday's law)

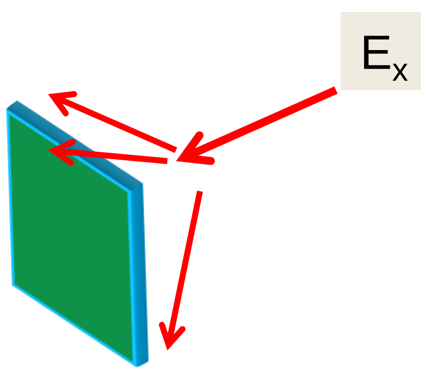

Resistive Anomaly
- current attempts to move around, above and below the resistor

Types of Anomalies: VLF TE weak conductor (effect of primary Ex).

In this example, the location of the structure was chosen such that the source Ex and Hy have weak gradients. The structure is offset from the survey line (lower left figure) to enable a response for all components of the H field.

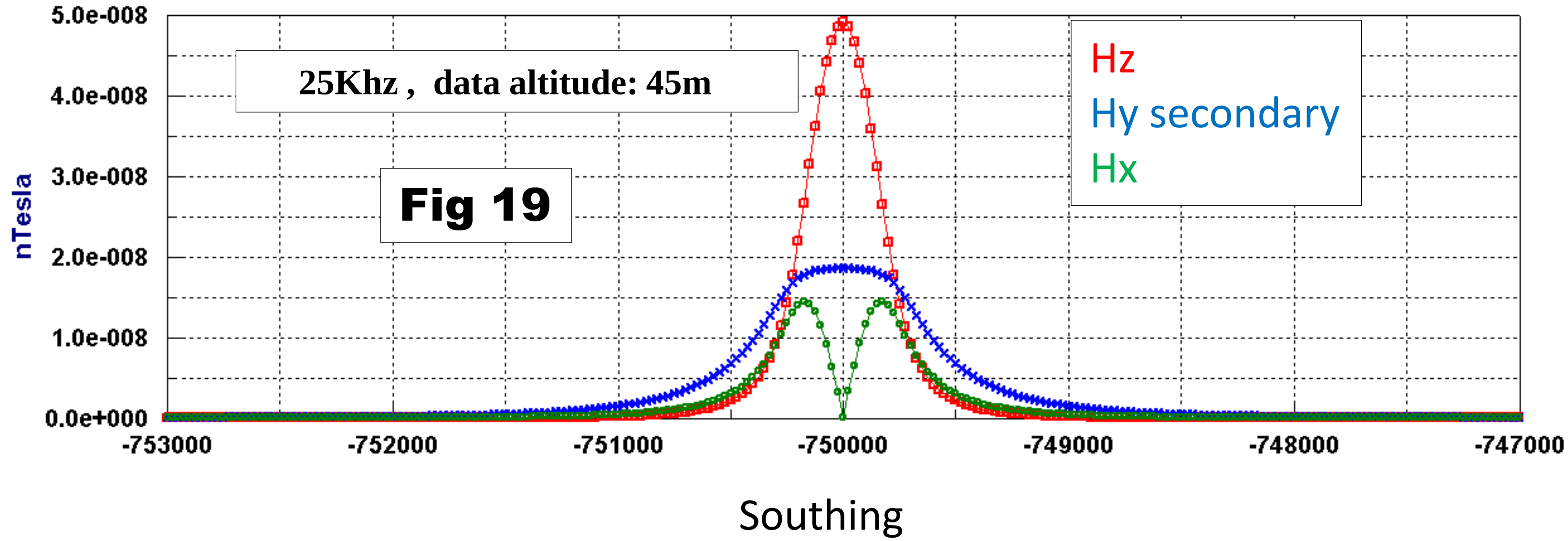

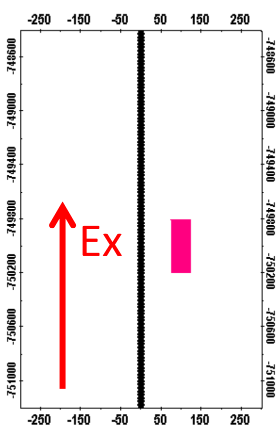

Strike – NS, (100,-750000)
Depth to top – 5m
Length – 400m
Width -   50m
Thickness - 400m
Offset from Profile - 100m
Resistivity – 50 Ωm
Background – 20K Ωm

If we were to derive tipper vectors then it must be a 2-vector.

$$H_z = T_{zx} H_x + T_{zy} H_y$$

Types of Anomalies: VLF TE weak conductor (effect of primary Ex).

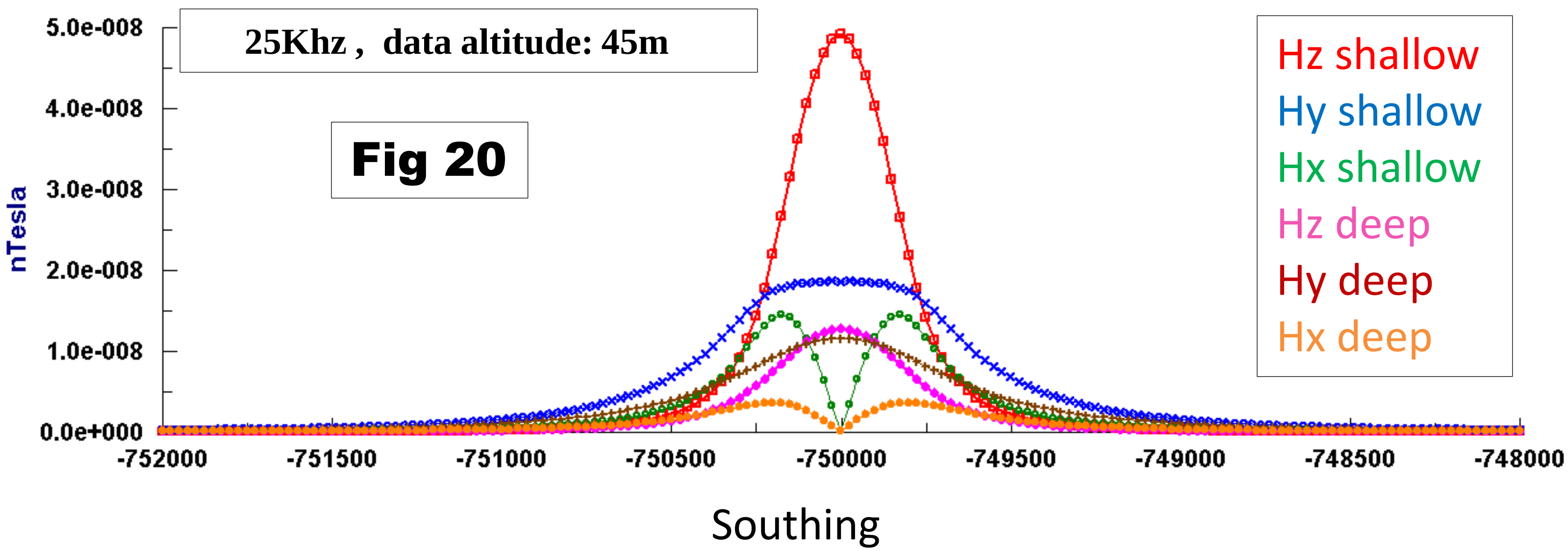

Strike – NS
Depth – 5m and 100m
Length – 400m
Width - 50m
Thickness - 400m
Resistivity – 50 Ωm
Background – 20K Ωm

In this example, the structure is the same as in the previous figure but we compare the response at 2 depths below ground. The shape of the responses is unchanged with depth of burial but the relative strengths, Hz:Hx and Hz:Hy change with depth.

Types of Anomalies: MT TE weak conductor (effect of primary Ex).

In this example, we compare the responses of the shallow structure (Figure21a) with a VLF source and an MT source (Figure21b). The responses are very similar. The amplitudes are not comparable as the source strength is not the same and in fact the MT source strength is in some sense arbitrary. Here, the source Hx = (1,0).

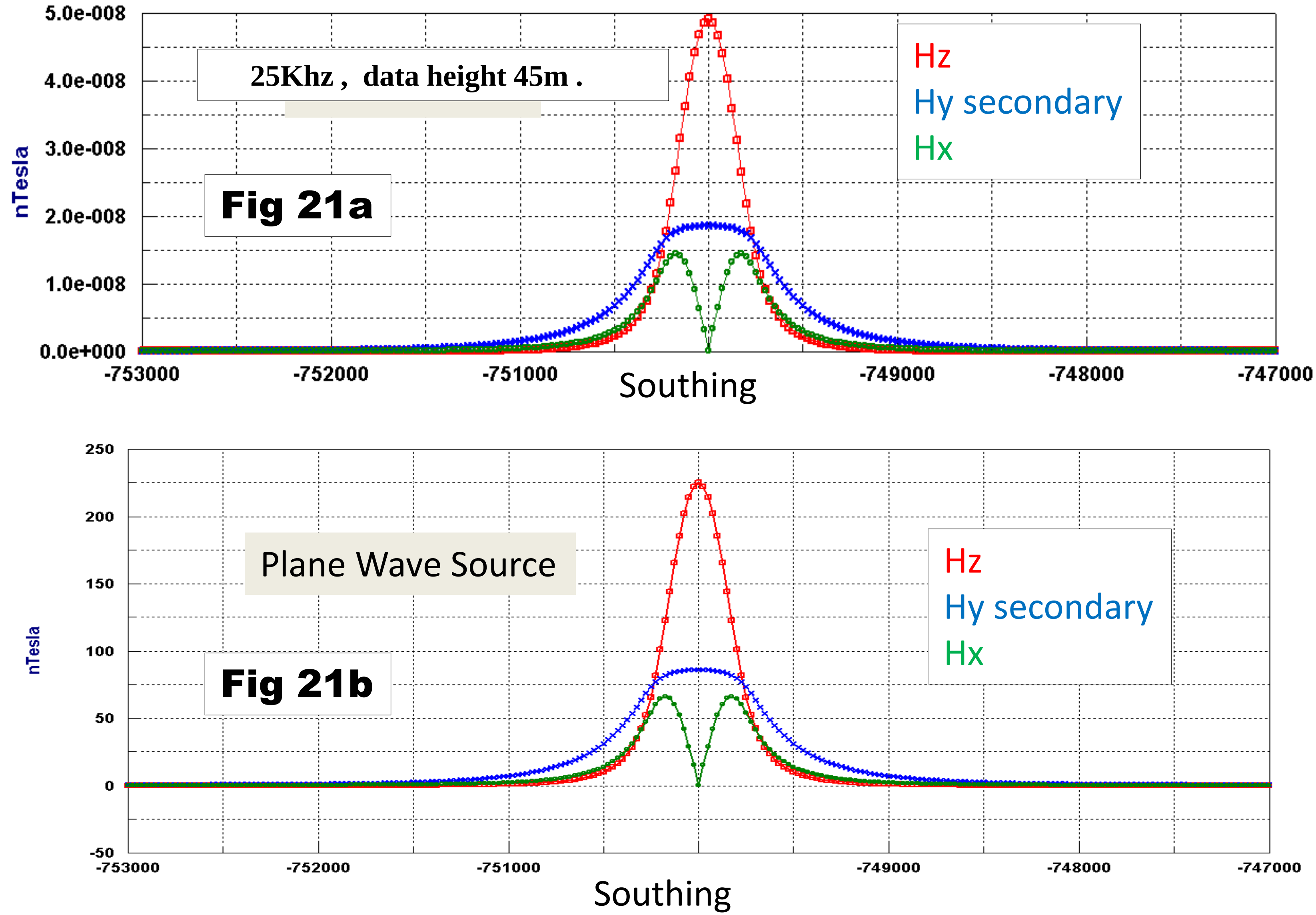

Types of Anomalies: MT TE weak conductor (effect of primary Ex).

In this example, we compare the shallow and deep structure (pg18) responses for the VLF and MT source fields.

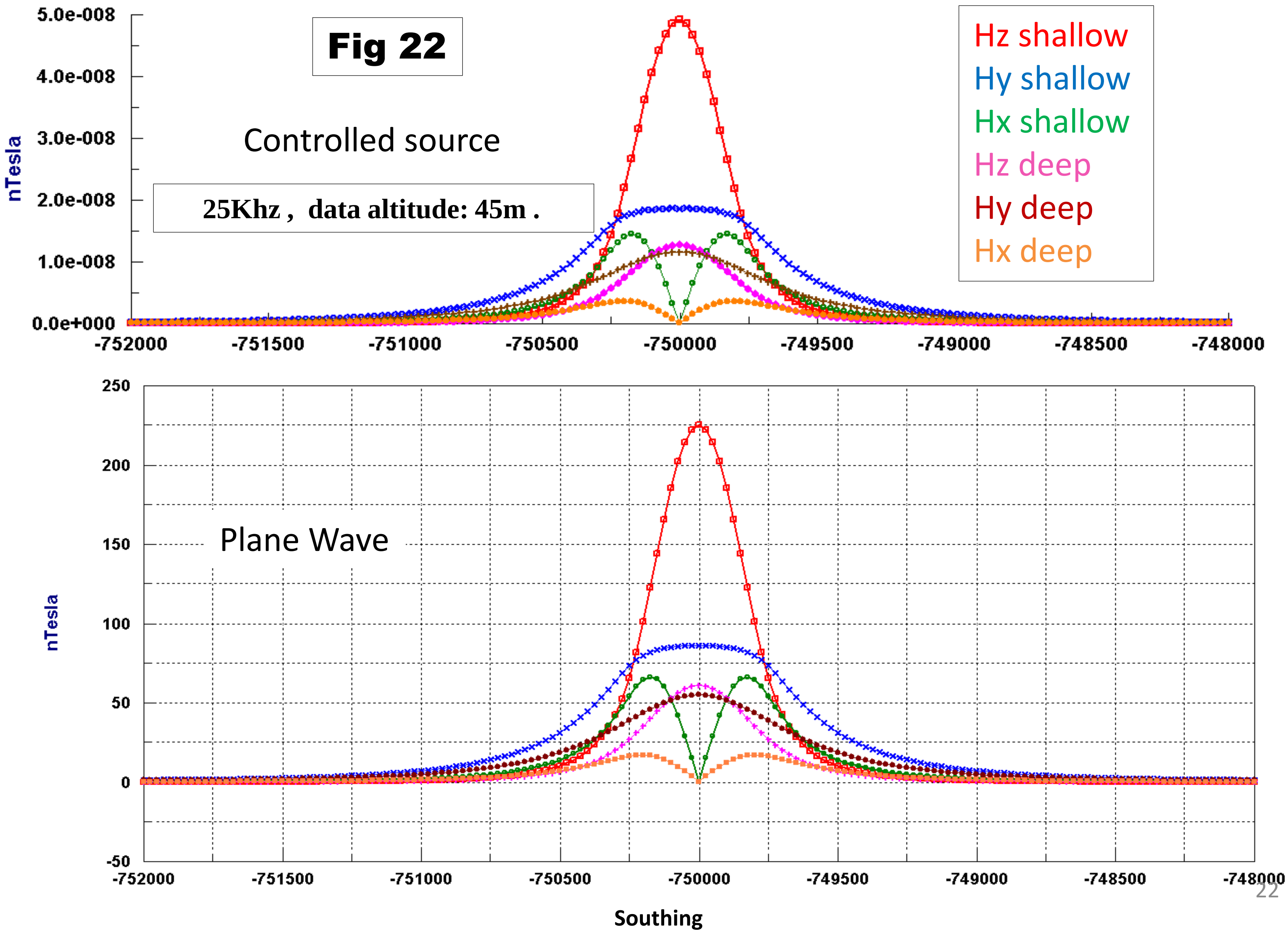

Types of Anomalies: VLF TE strong conductor (effect of primary Hy).

Again, we have chosen the anomaly location such that the sources Ex and Hy have weak gradients in the earth. Now, we use an inductive anomaly.

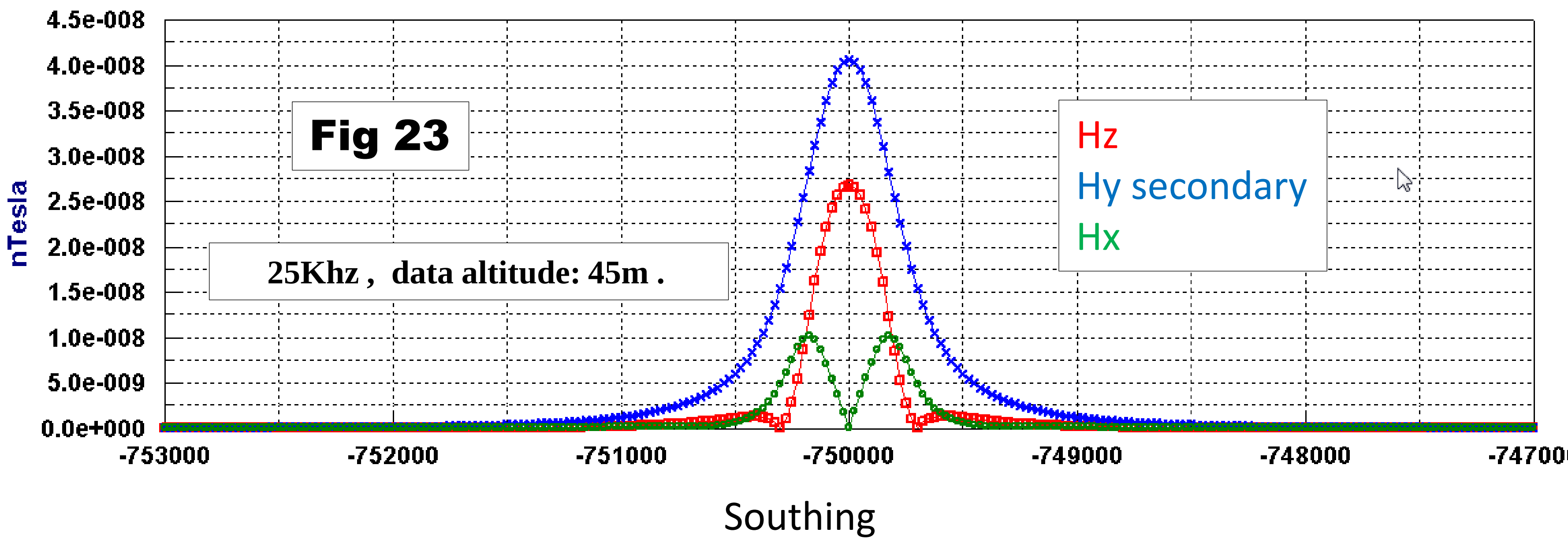

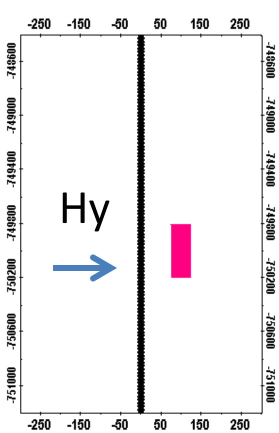

Strike – NS, (50,-750000)
Depth to top – 50m
Length – 400m
Width - “ thin sheet”
Thickness - 400m
Conductance – 160
Offset from Profile – 50m
Background – 20K Ωm
Dip - 60 degrees

$$H_z = T_{zx} H_x + T_{zy} H_y$$

Types of Anomalies: MT TE strong conductor (effect of primary Hy).

Magnetotelluric Response to the inductive anomaly of pg21.

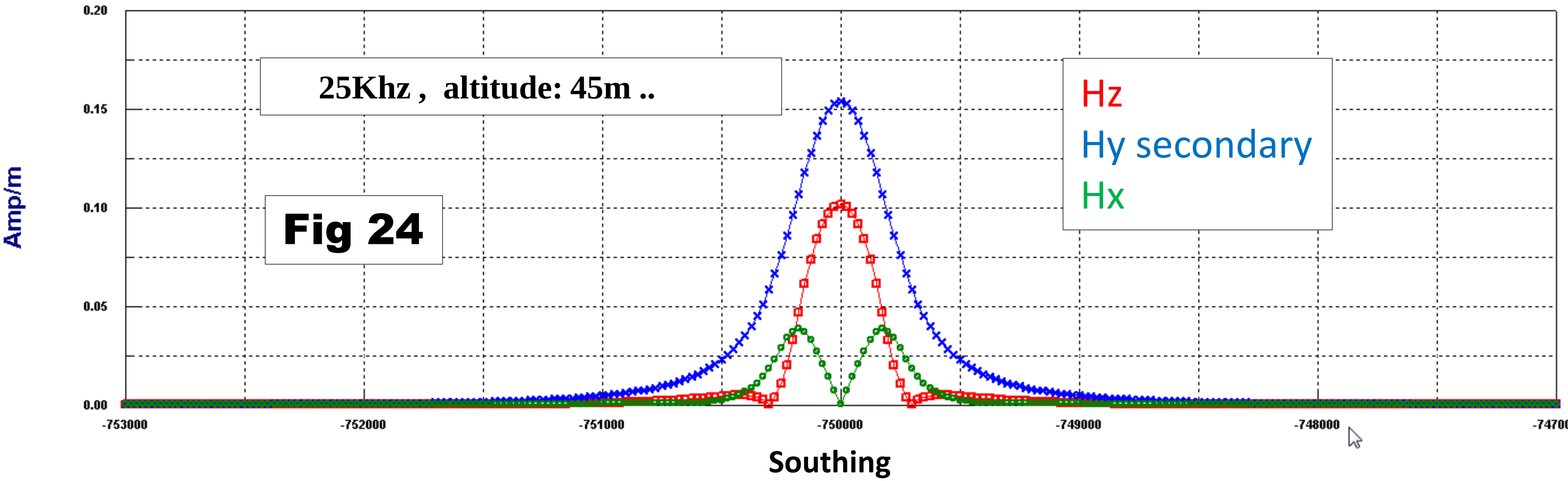

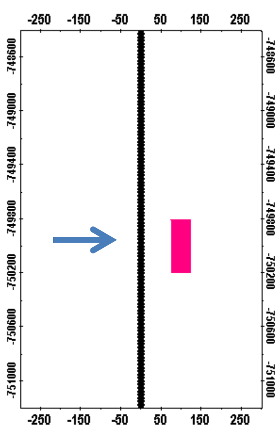

Strike – NS
Depth to top – 50m
Length – 400m
Width - thin sheet
Thickness - 400m
Conductance – 160 ohms
Offset from Profile – 50m
Background – 20K Ωm
Dip - 60 degrees

$$H_z = T_{zx} H_x + T_{zy} H_y$$

Types of Anomalies: MT vs VLF TE strong conductor (effect of primary Hy)

Chose location where VLF source Ex and Hy have weak gradients in the earth.

MT simulations have an arbitrary amplitude for the source strength. To compare, in detail, the ratio of the peak of Hz was determined for both sources and then all components and sites of the VLF data were normalized to this ratio.

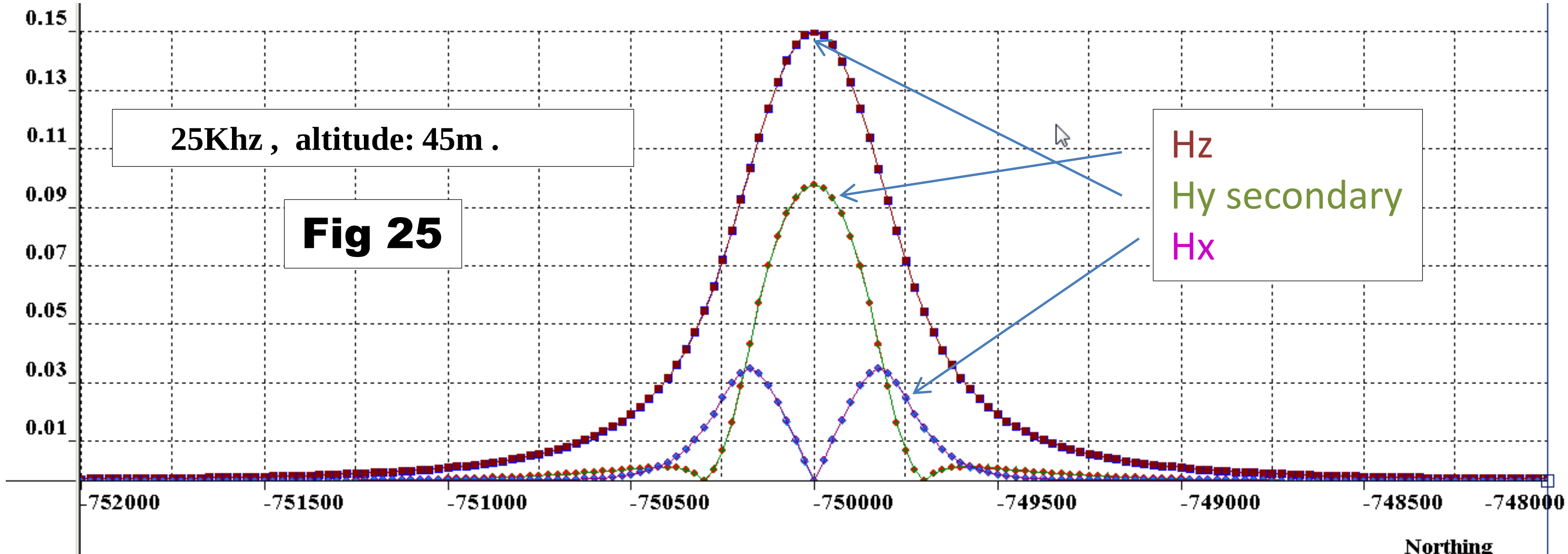

Strike – NS, (50,-750000)
Depth to top – 50m
Length – 400m
Width - thin sheet
Thickness - 400m
Conductance – 160
Offset from Profile – 50m
Background – 20K Ωm
Dip - 60 degrees

Figure 25 plots the 3 components of H for both the VLF and MT simulations. The results are not exactly equal but certainly within typical noise levels for surveys. { Solid lines connect VLF responses, symbols for both VLF and MT. *MT: Hz(Blue rombus , Hy (red rombus), Hx (blue rombus) }*

$$H_z = T_{zx} H_x + T_{zy} H_y$$

Types of Anomalies: MT, VLF TE Effect of Background Resistivity

From the same transmitter, transmitting with the same power, the primary fields within the ground are affected directly by the resistivity of the host rock. Below (Figure 26), is shown the Ex field in the direction of propagation immediately below the surface. The inphase and quadrature of this field is shown for two host resistivitiies and we see that the electric field is increased with increasing resistivity. Therefore, the Hz response of anomalies embedded in this host are directly affected by the host resistivities. Note that the center of the anomaly is at Southing = -735000 and thus the nature of the Bz response is different than in the previous results.

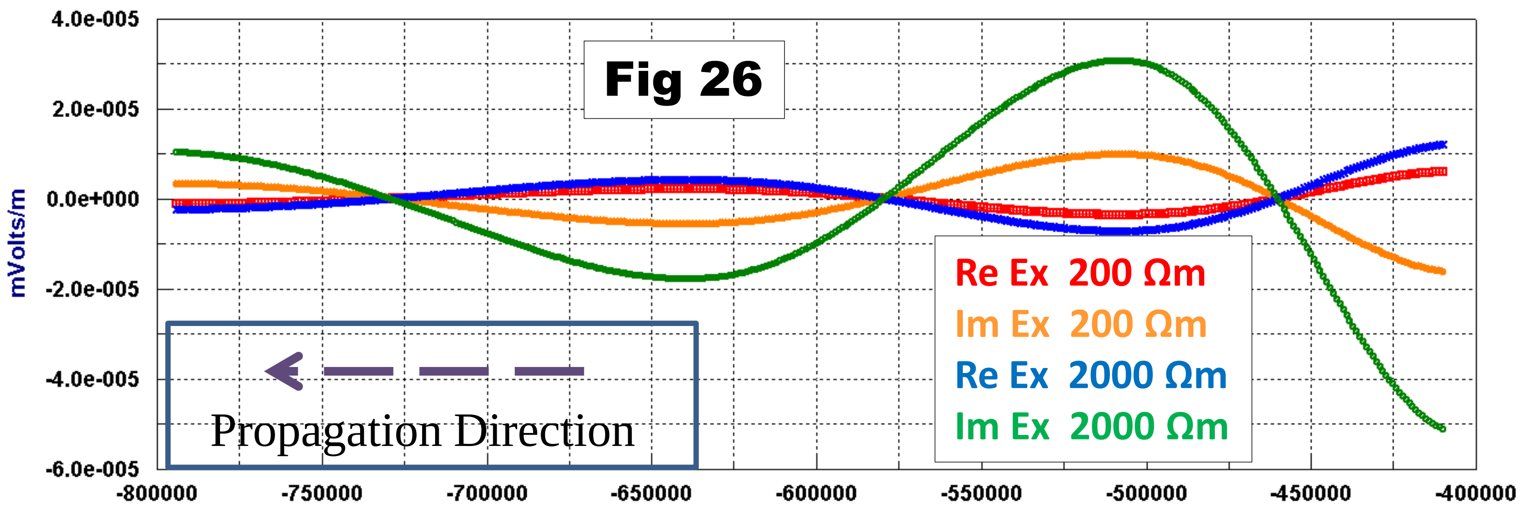

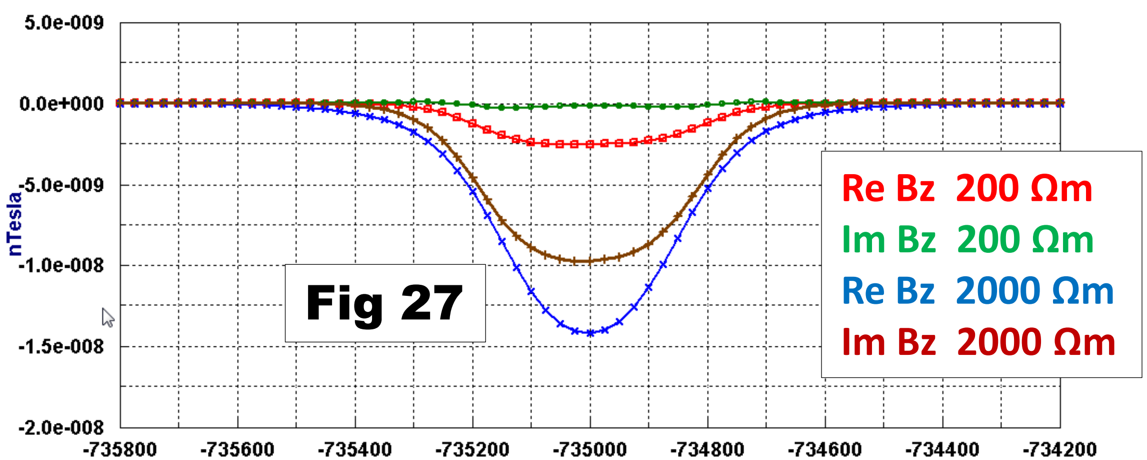

Figure 27 compares the Hz response at an altitude of 45m for the same anomaly to the source fields shown in Figure 26. The frequency of excitation is again 25Khz.

Strike – NS, (100,-735000)
Depth – 5m
Length – 400m
Width - 50m
Thickness - 400m
Resistivity – 50 Ωm

Errors Simulating VLF as plane wave: VLF TE weak conductor (effect of primary Ex)

Again for 25Khz at an altitude of 45m but this time the structure is located in a location where source the Ex and Hy have strong gradients in the earth. The same structure is located in 3 different locations as shown in the lower right figure. Figure 28 displays the inphase and quadrature of the Ex source field. All the specifics of the model are shown in the box on the lower left.

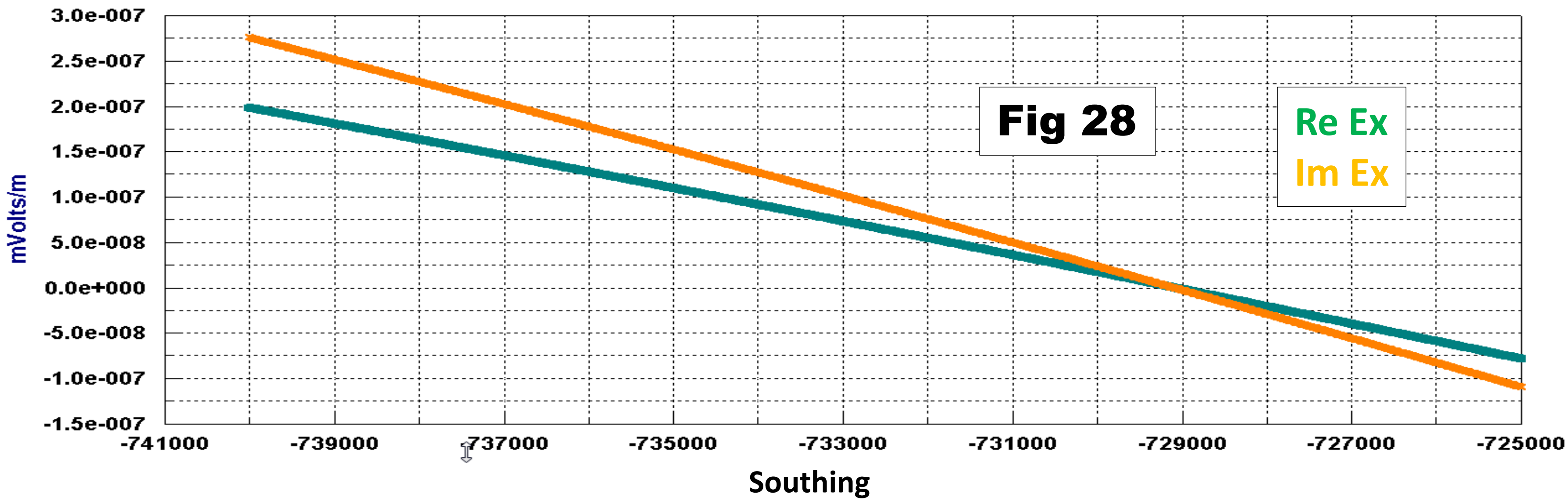

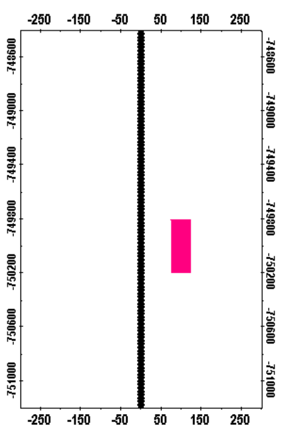

Strike – NS
Depth to top – 5m
Length – 400m
Width - 50m
Thickness - 400m
Offset from Profile - 100m
Resistivity – 50 Ωm
Background – 20K Ωm

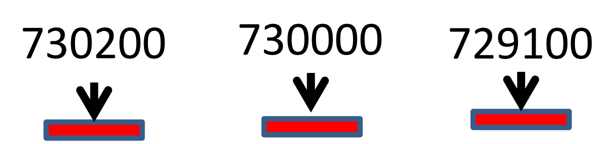

The three locations at different radial distances from the transmitter

Errors Simulating VLF as plane wave: VLF TE weak conductor (effect of primary Ex)

Hz responses at 25Khz and at an altitude of 45m .

We compare the results of simulating the weak conductor in an area where the primary source fields have strong gradients. The Hz total response is shown below for the 3 targets all with exactly the same properties but each at a different location as indicated bottom left.

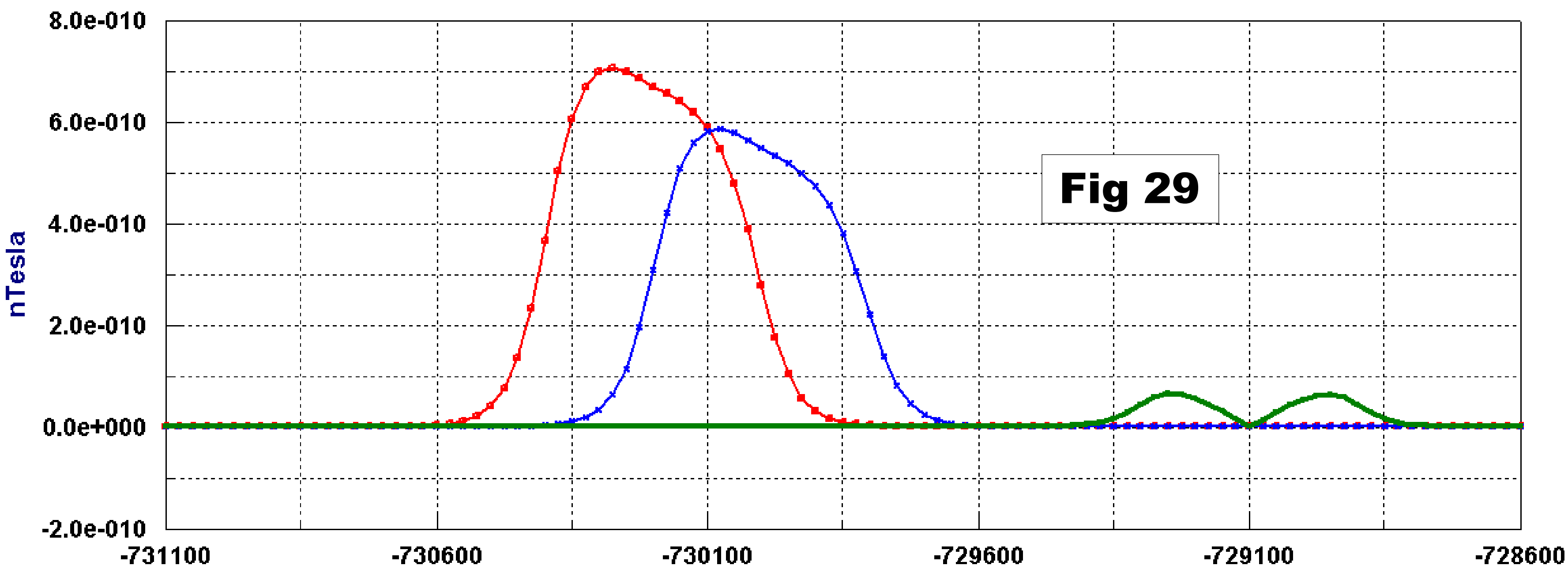

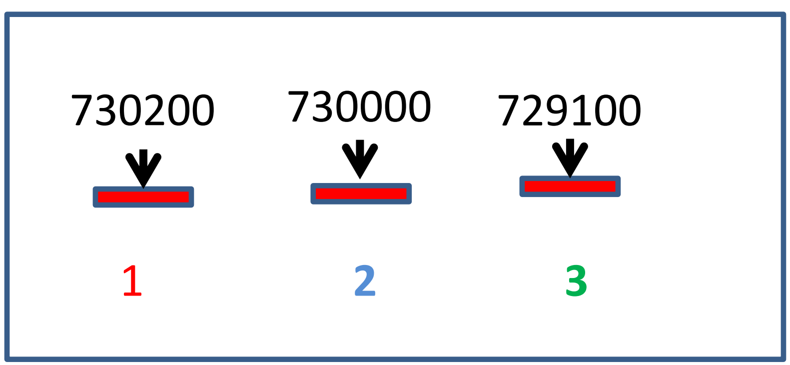

These responses are quite contrary to MT simulations which would produce the same results at each location. Of course, if the MT data is not processed with a remote station then 3D source effects could still remain in the source field and such results could occur in MT data. Note that in the case of ZTEM data, there is no remote processing and thus such data has to be considered questionable.

Can TIPPERS (induction vectors) from VLF Data be used with MT inversion algorithms?

In review for non-MT specialists: The calculation of tipper values from magnetotelluric data is a statistical procedure. The time series, of each measured field is broken into sections and the spectra of each section is calculated. The cross spectra are defined below. This method requires, for accuracy, many estimates of the data or independent realizations from the time series.

Computing Impedance Estimates from Auto and Cross Spectra

$$f(\omega) = \int f(t)\, e^{-2i\omega t}\, dt$$

$S(\omega) = f(\omega) f^*(\omega)$, power spectra or spectral density

Convolution and auto- and cross-correlation of random processes

$$h(t) = \int f(u) g^* (t-u)\, du$$

$h(\omega) = f(\omega) g^*(\omega)$, cross-spectra

$h(\omega) = f(\omega) f^*(\omega)$, auto-spectra

However, in MT, we utilize for spectra, a best estimate of the spectra, that is, for example

$EH(\omega) = {}^{1}/_{N} \sum_i e_i(\omega) h_i^*(\omega)$, cross-spectra

Where we have N slices of our time series

Induction or Tipper Vectors

Use of the remote data as indicated below helps assure unbiased estimates as well as helping to remove 3D source effects. The tipper equation is an assumed equation as there is no proof of this equation. It can be proven for a 2D structure but also if all the 3D structures have only galvanic excitations (Groom, 1988). Also, it is assumed that the tipper vector (Ax,Ay) has a unique solution for each station.

If we define the induction vector as (Ax,Ay) then

$$Hz = AxHx + AyHy$$

If Hx and Hy are chosen as the reference field then

$$Hz \cdot Hx = Ax\ Hx \cdot Hx + Ay\ Hy \cdot Hx$$

$$Hz \cdot Hy = Ax\ Hx \cdot Hy + Ay\ Hy \cdot Hy$$

Thus the matrix, T, is unchanged and

$$\begin{bmatrix} Ax \\ Ay \end{bmatrix} = T^{-1} \begin{bmatrix} Hz \cdot Hx \\ Hz \cdot Hy \end{bmatrix}$$

Similarly, if remote fields are utilized, the inverse operator is unchanged from that for obtaining the impedance elements.

$$Det(T) = (Hx \cdot H^R x)(Hy \cdot H^R y) - (Hy \cdot H^R x)(Hx \cdot H^R y)$$

And the inverse

$$T^{-1} = \frac{1}{Det(T)} \begin{bmatrix} Hy \cdot H^R y & -Hy \cdot H^R x \\ -Hx \cdot H^R y & Hx \cdot H^R x \end{bmatrix}$$

Induction or Tipper Vectors calculations for MT sources

The purpose of the MT processing procedures to calculate tippers is to have a sufficiently large number of data samples to try to ensure that the variations in the source field have been averaged to a relatively uniform wave with no specific source field polarization. For the MT situation, as the processing tries to remove all 3D source effects and to have only plane wave source fields, we could expect that there exists this linear transformation between the horizontal and vertical fields and the transformation vector (matrix) is unique. If all the source fields are plane waves during a given measurement then every 2-vector source event will be a linear combination of any chosen orthogonal bases for the set of all source fields. This would imply uniqueness of the tipper vectors.

For synthetic data whether in forward modeling or inverse modeling, statistical procedures are not practical and so the technique normally utilized to implement the calculation of the tippers is to simulate the model with two source independent polarizations which are normally chosen to be orthogonal.

If this linear transformation (Eqn 1) between the horizontal and vertical magnetic field exists then the two polarizations need not be orthogonal but must be independent. As the equations below show, the amplitudes of the source fields from each polarization need not be equal. While, we have not proved that T_x and T_y are unique at each station independent of the source polarizations, we have performed numerous simulations to show that for both channelling and inductive 3D responses, that the source polarizations need simply be independent and need not be orthogonal to produce a result independent of polarization. These latter results are important for VLF, if we wish to use MT algorithms . For, it is not possible in practise in VLF, to use orthogonal source polarizations nor sources which have equal strength.

$$\mathbf{H^i_z = T_x H^i_x + T_y H^i_y, \quad i=1,2 \quad (Eqn\ 1)}$$

thus

$$H^1_z H^2_y = T_x H^1_x H^2_y + T_y H^1_y H^2_y$$

$$H^2_z H^1_y = T_x H^2_x H^1_y + T_y H^2_y H^1_y$$

thus

$$T_x = H^1_z H^2_y - H^2_z H^1_y \,/\, [H^1_x H^2_y - H^2_x H^1_y]$$

$$T_y = H^2_z H^1_x - H^1_z H^2_x \,/\, [H^1_x H^2_y - H^2_x H^1_y]$$

For synthetic data, depending on numerical algorithm stability more than 2 polarizations may be required.

Tipper Vectors Uniqueness for MT sources

$$H^i_z = T_x H^i_x + T_y H^i_y, \quad i=1,2 \quad \text{(Eqn 1)}$$

thus

$$H^1_z H^2_y = T_x H^1_x H^2_y + T_y H^1_y H^2_y$$
$$H^2_z H^1_y = T_x H^2_x H^1_y + T_y H^2_y H^1_y$$

thus $T_x = H^1_z H^2_y - H^2_z H^1_y / [H^1_x H^2_y - H^2_x H^1_y]$ (1)

$T_y = H^2_z H^1_x - H^1_z H^2_x / [H^1_x H^2_y - H^2_x H^1_y]$

In this proof, we assume theoretical MT source fields to be uniform plane waves where $[\hat{E}_0 \times \hat{H}_0]$ propagate vertically downward within the media beneath the air. In which case, we may define two orthogonal basis functions for the source fields: $H_x^0\,\hat{\mathbf{x}}$ and $H_y^0\hat{\mathbf{y}}$. $(\hat{\mathbf{x}},\hat{\mathbf{y}})$ are arbitrary orthogonal unit vectors.

Thus, any source field, H_s^i, can be defined as a linear combination of the basis functions

$H_s^i = a_i H_x^0\,\mathbf{x} + b_i H_y^0\mathbf{y}$ and the associated vertical field induced by, H_s^i ,is therefore $H_z^i = a_i\, {}_xH_z^0 + b_i\, {}_yH_z^0$ (2)

where, ${}_xH_z^0$ is the vertical field induced by the basis function, H_x^0 and ${}_yH_z^0$ that induced by the basis function, H_y^0.

Thus, the tippers for the basis sources are,

$$T_x = {}_xH_z^0 / H_x^0$$
$$T_y = {}_yH_z^0 / H_y^0$$

And substituting two sources fields, H_s^1 and H_s^2 in expression (1) expressed as linear combinations of the source basis vectors (2) gives,

$$T_x = b_2 H^1_z - b_1 H^2_z / H_x^0 (a_1b_2 - a_2b_1)$$
$$T_y = a_2 H^2_z - a_1 H^1_z / H_y^0 (a_1b_2 - a_2b_1)$$

Substituting, $H_z^i = a_i\, {}_xH_z^0 + b_i\, {}_yH_z^0$, i=1,2 into the above expressions

$$T_x = (a_1b_2 - a_2b_1)\, {}_xH_z^0 / H_x^0 (a_1b_2 - a_2b_1) = {}_xH_z^0 / H_x^0$$
$$T_y = (a_1b_2 - a_2b_1)\, {}_yH_z^0 / H_y^0 (a_1b_2 - a_2b_1) = {}_yH_z^0 / H_y^0$$

This proves that for theoretical source fields that the MT tippers are unique whether measured on the ground or in the air. However, this proof does not work for the VLF fields as the source fields cannot form a 2-dimensional vector space. The same conclusion is true if there exists 3D source effects in MT data or airborne MT tipper data.

Verification of Numerical Tipper Vectors for MT Sources

Calculation of tippers for VLF sources may be an entirely different matter. Of course, for synthetic data, we can chose two orthogonal source. But, it can be difficult to collect data from two transmitters which are closely orthogonal in their polarizations. But, even given a limited number of locations where one could use two orthogonal polarizations, the source electric and magnetic fields will not have the same strength from the two antennae even when the antennae have the same source strength nor the same phase at the transmitted frequency. What are the possible results with VLF data ?

For, these MT tipper calculations, we utilize our standard thin conductor just off the survey line. The figure on the left utilizes the first electric source polarization as 45 degrees east of north and the second 45 degree west of north. The 2nd figure below utilizes the first polarization as north and the second directed northeast. Other source polarizations produce the same results as long as the polarizations are independent vectors. That is, the two sources must not be parallel. In Figure 30, these calculations are for stations at 45m above the ground. Calculations for ground stations are equally identical within a small computational difference. This is more a verification of our numerical accuracy as we have already proved that given the assumptions in interpreting MT, that the tipper vectors are unique at each location.

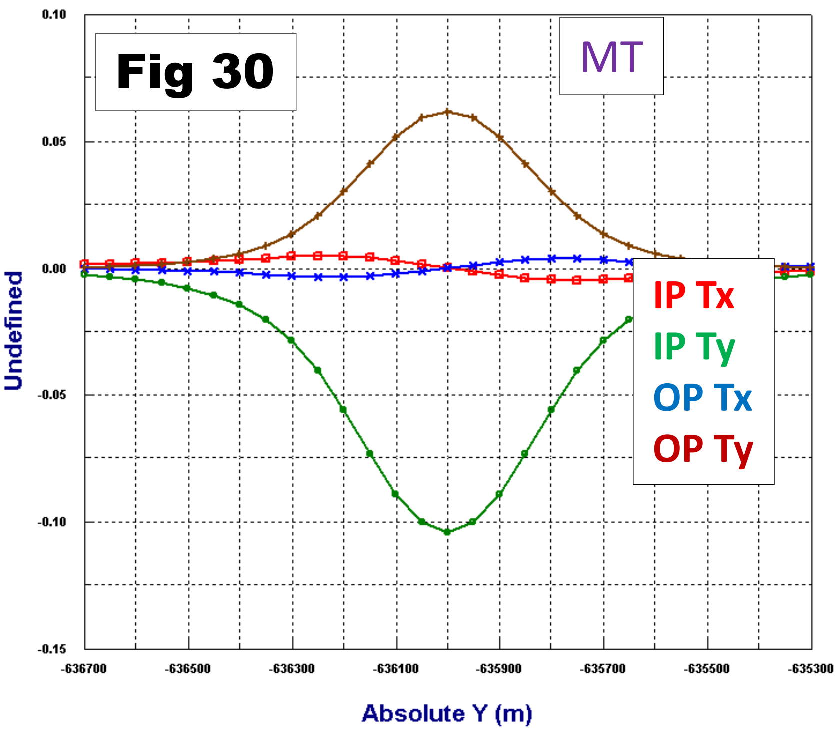

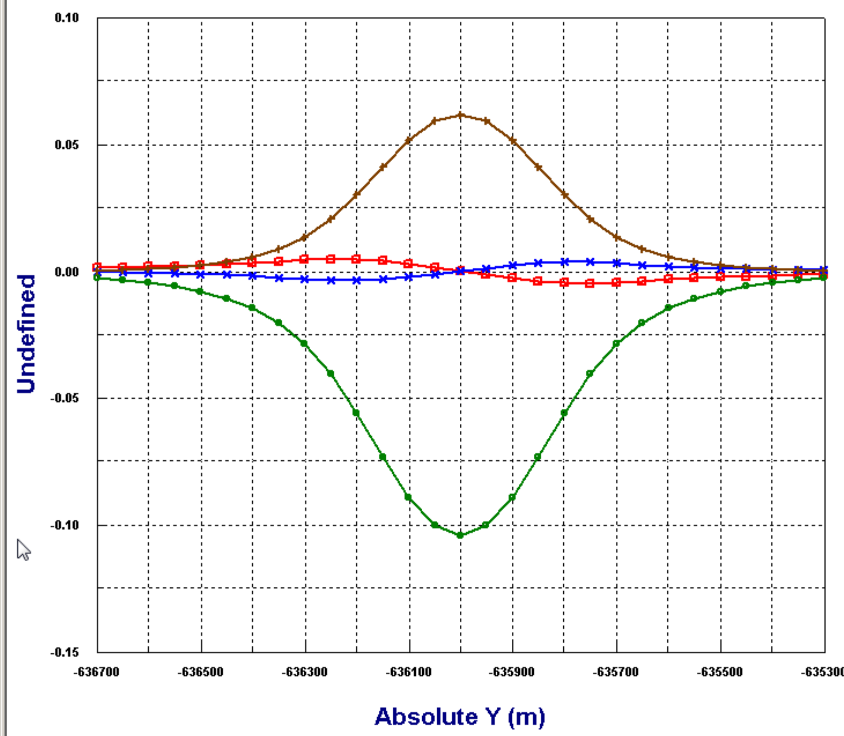

Induction or Tipper Vectors for VLF Sources

In the example below, the same model was utilized. The MT tippers are on the left. The VLF tippers, on the right, are calculated using the same equations. One VLF source was due north of the target and the other due east. Both sources are an equal distance from the target (650km). The results below on the left and right are similar in shape but the VLF results are much smaller than the MT results. There are other differences as well but another major difference is in the shape of T_x. The two VLF transmitters had the same emission strength.

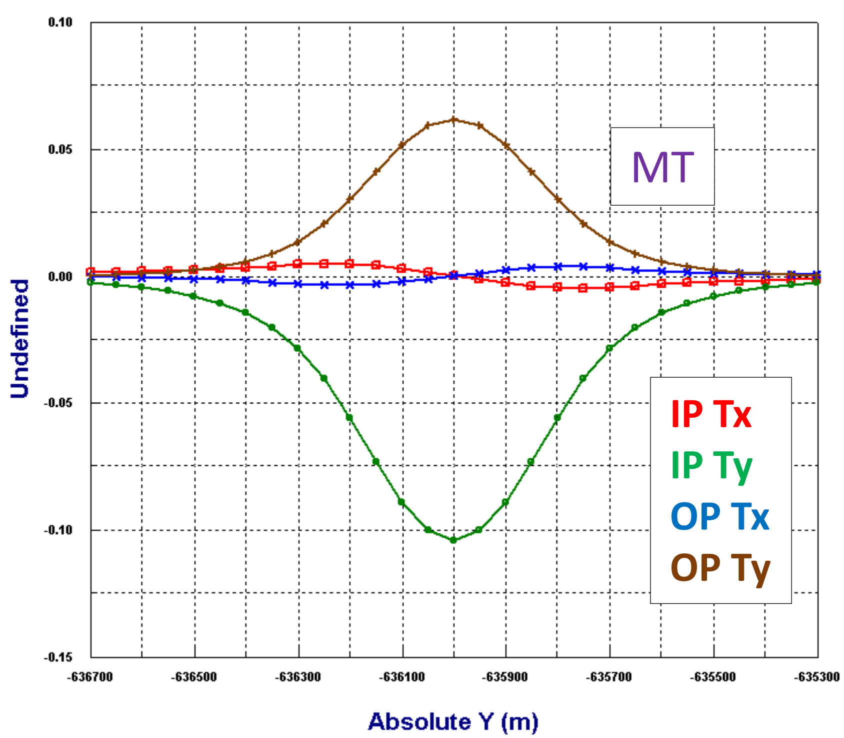

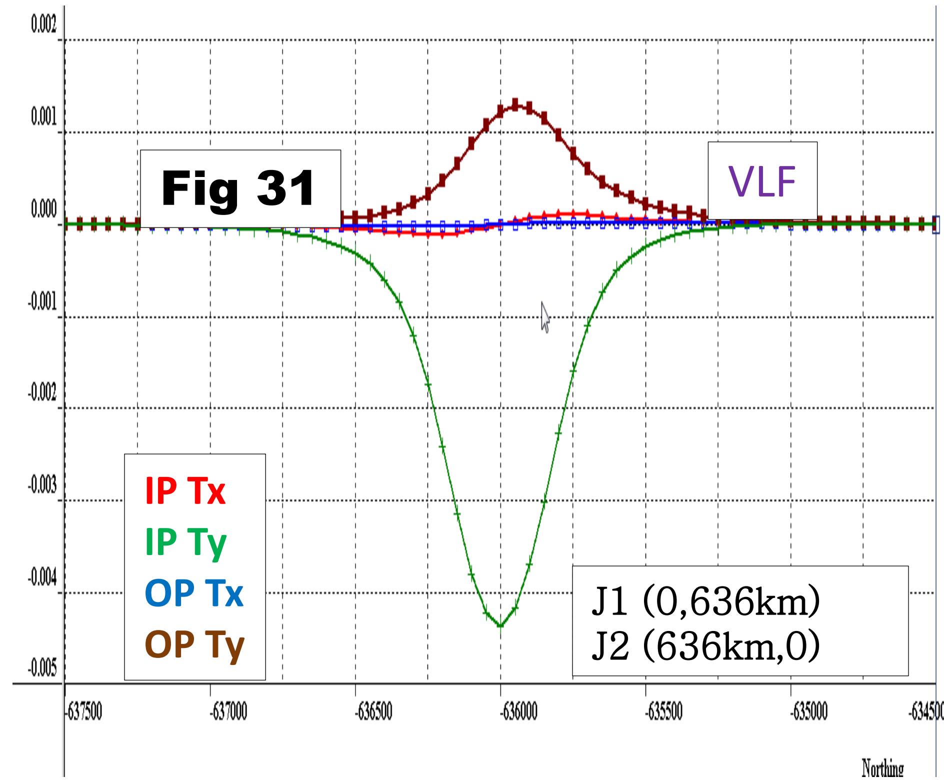

Induction or Tipper Vectors for VLF Sources

Studies :

1. Are VLF tipper vectors equal to MT tipper vectors ?
2. Are VLF tippers unique with regard to the location of the transmission antennae?

Study 1: **a) ground measurements** b) measurements in air 25Khz

For the VLF simulations, the transmitters are similarly 100m long, vertical in the air. In this example, one transmitter is 600km south of the target and the other 400km to the east of the target. The receivers are at ground level. The location of the target and sources were chosen, in this case, such that the background electric and magnetic fields in the ground at the target have very low gradients. The differences between the MT and VLF results are less than 1 part in a 1000. It should be noted that the algorithms are quasi-analytic to calculate the secondary field thus providing very high accurate secondary field calculations.

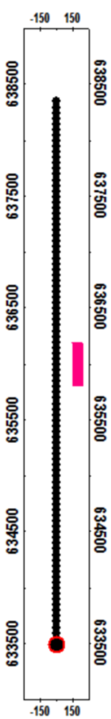

Fig 32

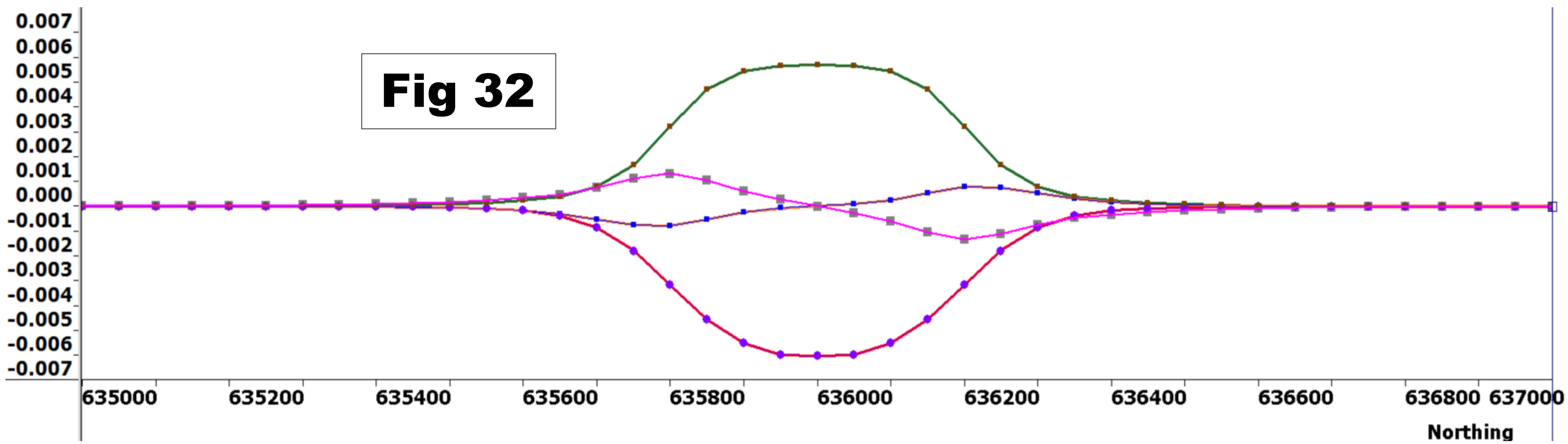

Strike – NS
Depth to top – 5m
Length – 400m
Width - 100m
Thickness - 100m
Offset from Profile - 200m
Resistivity – 1 Ωm
Background – 200 Ωm
Centre Point NS - 636000

--MT T_x Re | •VLF T_x Re
--MT T_x Im | •VLF T_x Im
--MT T_y Re | •VLF T_y Re
--MT T_y Im | •VLF T_y Im

Uniqueness Tipper Vectors for VLF Sources

Studies :

1. Are VLF tipper vectors equal to MT tipper vectors ?
2. Are VLF tippers unique with regard to the location of the transmission antennae?

Study 1: **a) ground measurements** b) measurements in air 25Khz

For measurements on the ground, we have found by simulating numerous pairs of transmitters that the VLF tippers appear often to be unique at each location. As one example, the figure below compares the VLF tippers for 2 pairs of sources. The first (S1) as mentioned on the previous page and the second (S2) has one transmitter 300km West and 500km South of the target while the other source is 450km East and 150km South. Solid lines are one set of sources while the plot symbols are for the other source.

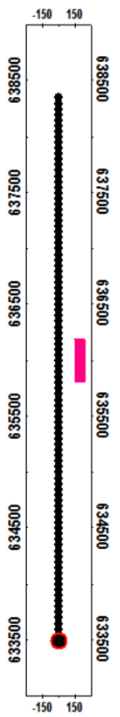

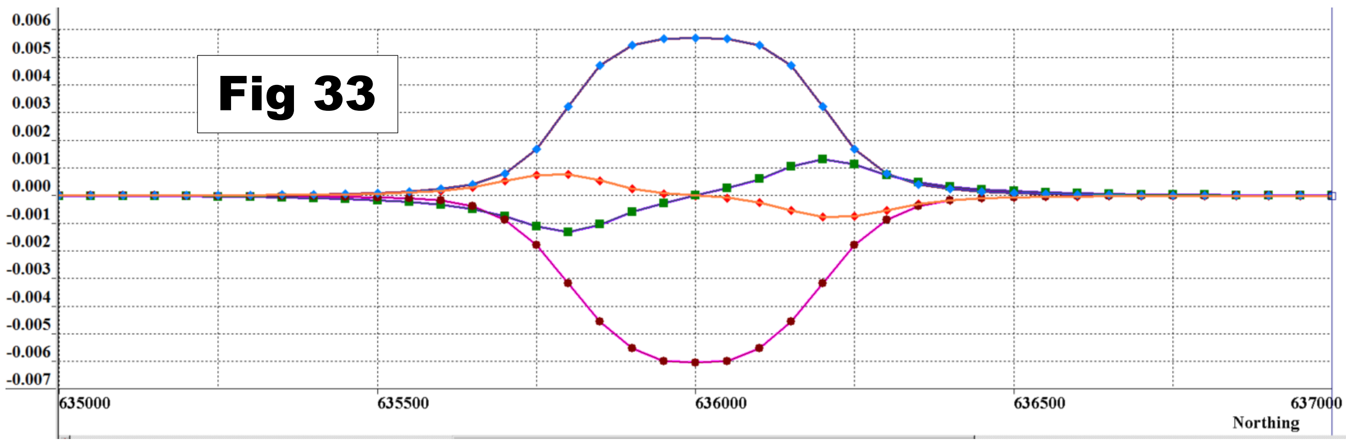

Strike – NS
Depth to top – 5m
Length – 400m
Width - 100m
Thickness - 100m
Offset from Profile - 200m
Resistivity – 1 Ωm
Background – 200 Ωm
Centre Point NS - 636000

Uniqueness Tipper Vectors for VLF Sources

Studies :

1. Are VLF tipper vectors equal to MT tipper vectors ?
2. Are VLF tippers unique with regard to the location of the transmission antennae?

Study 1: **a)** ground measurements b) **measurements in air** 25Khz

However, in the air, the VLF tippers seldom repeat with different source locations. Below is the same model as in Figures 32 and 33. But, in this case, the source locations are the same but now the measurements are 45m above ground. The differences between the 2 sets of tippers for the air from the 2 sets of sources can be most readily seen by the differences in the phases of the tipper elements. In the figure below, the results for Source 1 are marked by square symbols and for Source 2 by circular symbols.

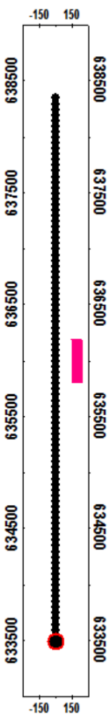

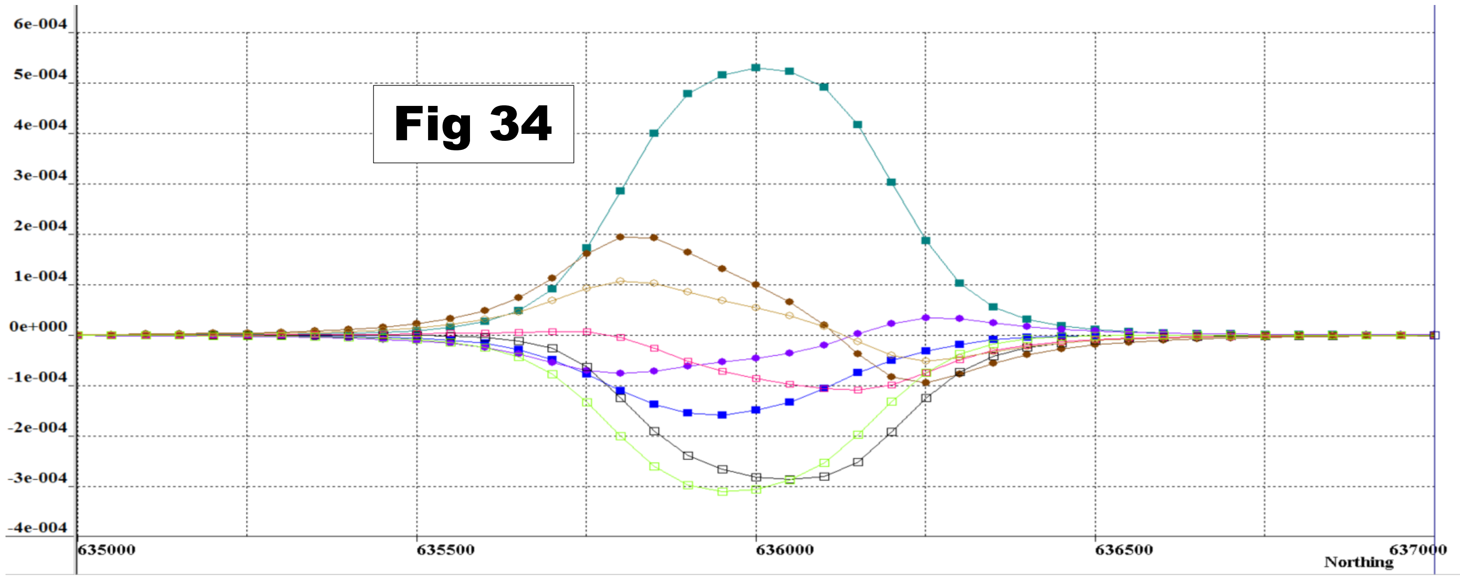

Fig 34

S1 -	S2
T_x Re	T_x Re
T_x Im	T_x Im
T_y Re	T_y Re
T_y Im	T_y Im

Strike – NS, Depth to top – 5m, Length – 400m
Width - 100m, Thickness - 100m, Offset from Profile - 200m
Resistivity – 1 Ωm , Background – 200 Ωm ,Centre Point NS - 636000

Induction or Tipper Vectors for VLF Sources

Studies :

1. Are VLF tipper vectors equal to MT tipper vectors ?
2. Are VLF tippers unique with regard to the location of the transmission locations?

Study 1: **a)** ground measurements b) **measurements in air** 25Khz

Even in regions of low VLF source gradients, the MT and VLF tippers can be different. For measurements in the air, we have found that the tippers are not unique with regard to the sources. In the example below, the VLF sources are as in the previous figure and the measurements are at 45m above the ground. It is important to remember that Hz has its source under the earth at the anomaly whereas the Hx and Hy are principally due to the 3D source interacting with the overall resistivity of the ground. Here, the MT and VLF tippers clearly differ greatly. Here, the main MT tipper elements are the imaginary potions of Tx and Ty and these greatly exceed any element in the VLF tippers.

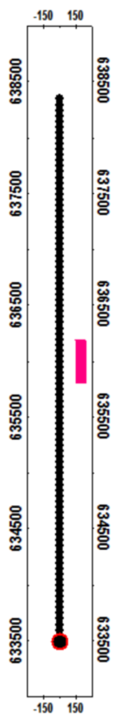

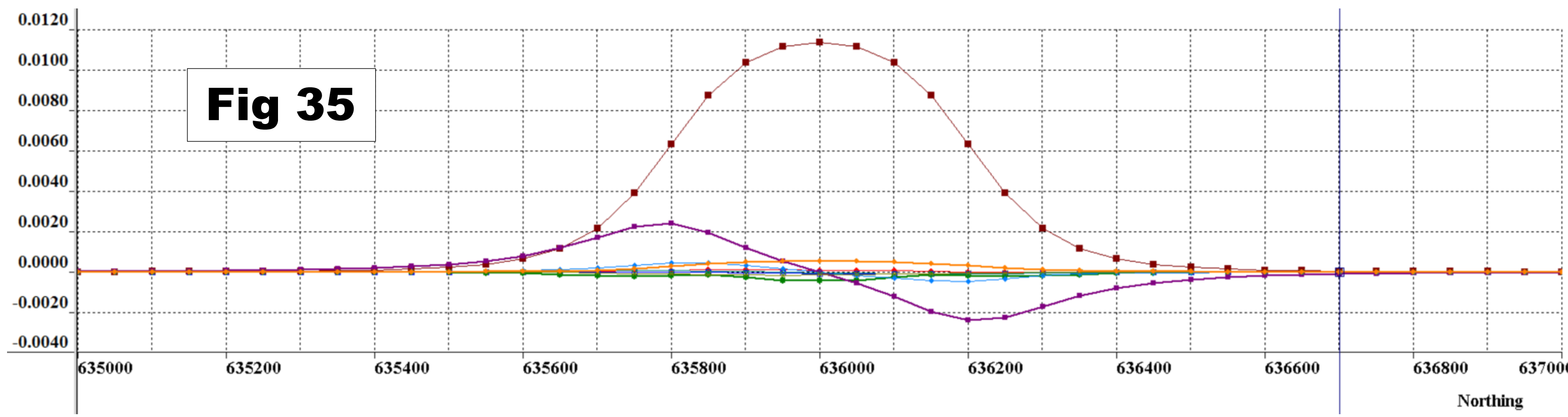

Strike – NS
Depth to top – 5m Length – 400m
Width - 100m Thickness - 100m
Offset from Profile - 200m
Resistivity – 1 Ωm Background – 200 Ωm
Centre Point NS - 636000

MT T_x Re | VLF2 T_x Re
MT T_x Im | VLF2 T_x Im
MT T_y Re | VLF2 T_y Re
MT T_y Im | VLF2 T_y Im

Induction or Tipper Vectors for VLF Sources vs MT sources

Studies :

1. Are VLF tipper vectors equal to MT tipper vectors ?
2. Are VLF tippers unique with regard to the location of the transmission antennae?

Study 1: **a)** ground measurements b) **measurements in air** 25 Khz

For the same model but now at a height of 45m above the ground, there are now virtually no comparison between the VLF results and the MT results. We show only the 2 major MT components with comparison to their VLF values.

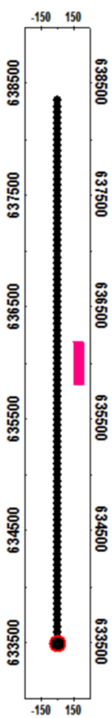

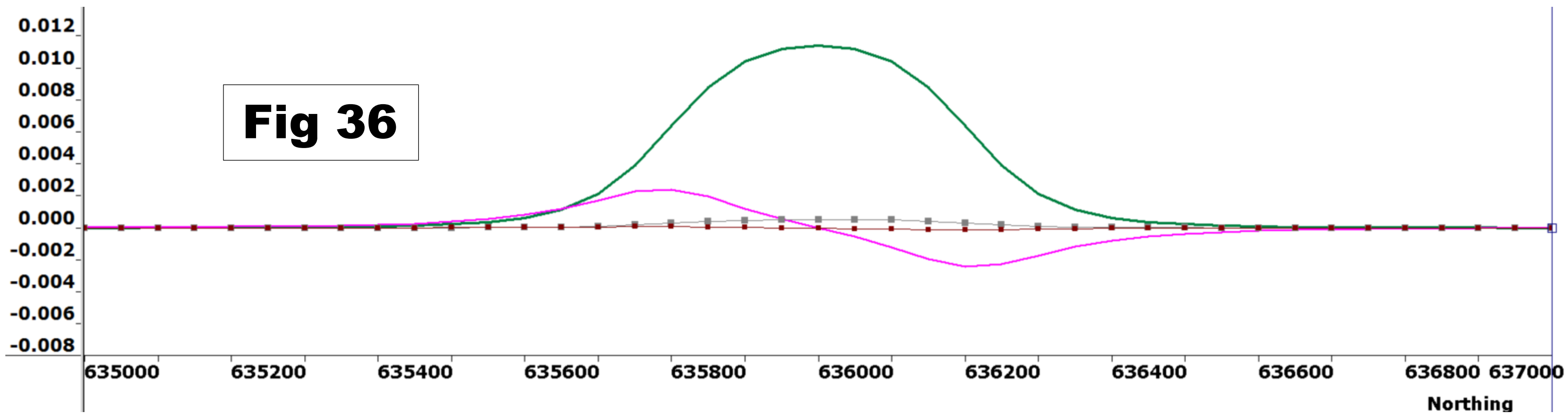

Strike – NS
Depth to top – 5m
Length – 400m
Width - 100m
Thickness - 100m
Offset from Profile - 200m
Resistivity – 1 Ωm
Background – 200 Ωm
Centre Point NS - 636000

--MT T_x Im | •VLF T_x Im
--MT T_y Im | •VLF T_y Im

Uniqueness Tipper Vectors for VLF Sources

Study : Longer strike and greater depth extent, more resistive ground, symmetrical w.r.t. X and Y axes

1. Location of anomaly: Gradients in VLF source fields

Study 2: **a) ground measurements** b) measurements in air 25Khz

In this example, we have a much larger object both in length (4km) and in depth 800m. In this case, the object is roughly symmetrical to NS and EW polarization. Thus, we would expect Tx ≈ Ty. The anomaly is slightly more to the east than west and thus exact symmetry may not be seen but in the figure below for MT, Tx and Ty are indeed almost identical (Figure 37a). The VLF results are similar but the only element that matches the MT closely is Im(Ty) but the Re(Ty) results are quite similar.

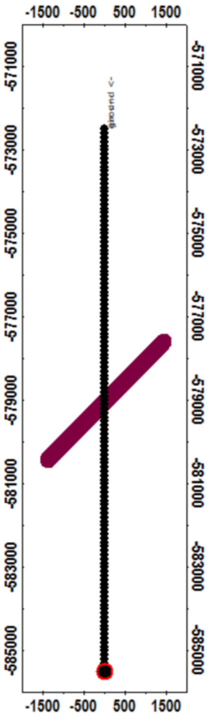

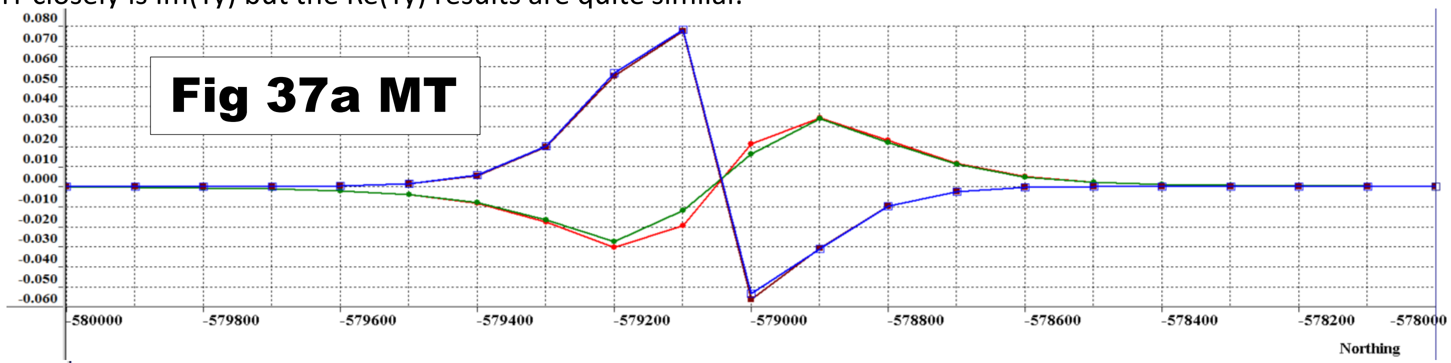

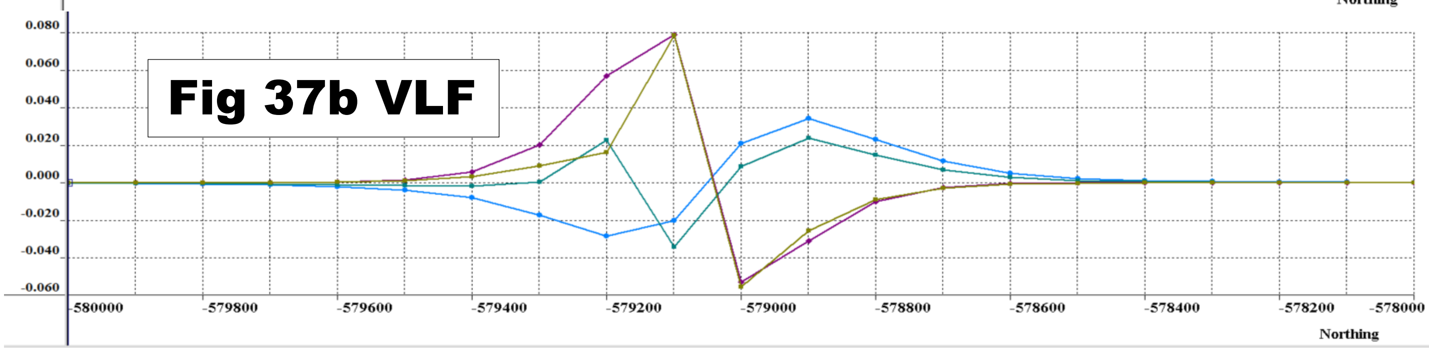

Strike – 45NE, Depth to top – 10m, Length – 4km, Width - 25m, Thickness - 800m, Offset from Profile - 0m, Resistivity – 2.5 Ωm , Background – 800 Ωm ,Centre Point NS - -579000

MT T_x Re	VLF T_x Re
MT T_x Im	VLF T_x Im
MT T_y Re	VLF T_y Re
MT T_y Im	VLF T_y Im

Uniqueness Tipper Vectors for VLF Sources

Study : Longer strike and greater depth extent, more resistive ground, symmetrical w.r.t. X and Y

1. Strong gradients in VLF source fields

Study 2: **a) ground measurements** b) measurements in air 25Khz

We now compare the tippers produced by two pairs of vertical current sources. In the first case, shown in both Figure 37b and 38a, one source is 600km north of the target and the other 400km east of the target while in the other case (Figure38b), the second source is 500km west of the target and 100km north of the target. In this case, the VLF tippers are not unique. This is because the VLF source fields are not both approximately uniform at the anomaly. This indicates a problem not just for both airborne and ground VLF to interpret using MT software.

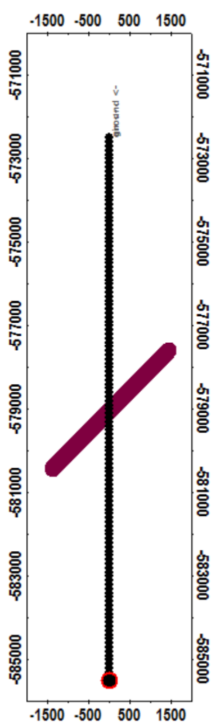

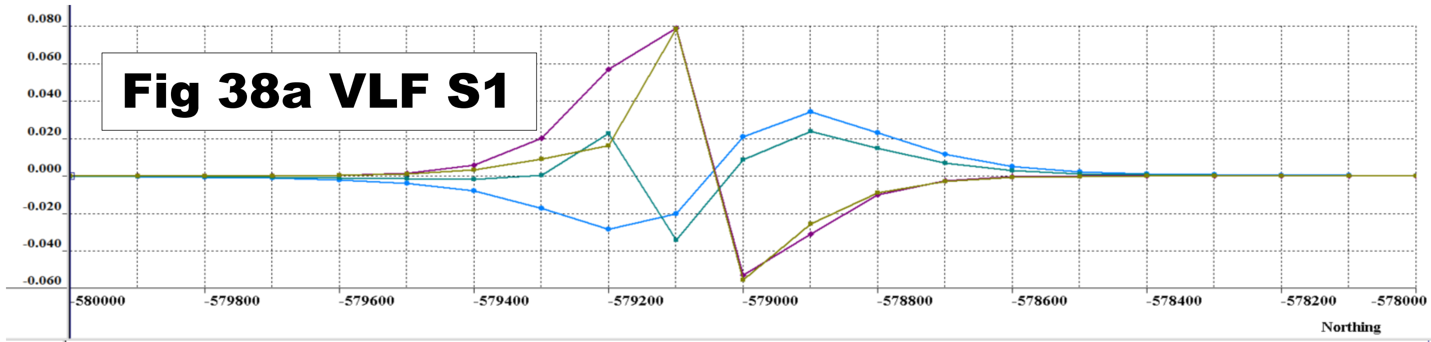

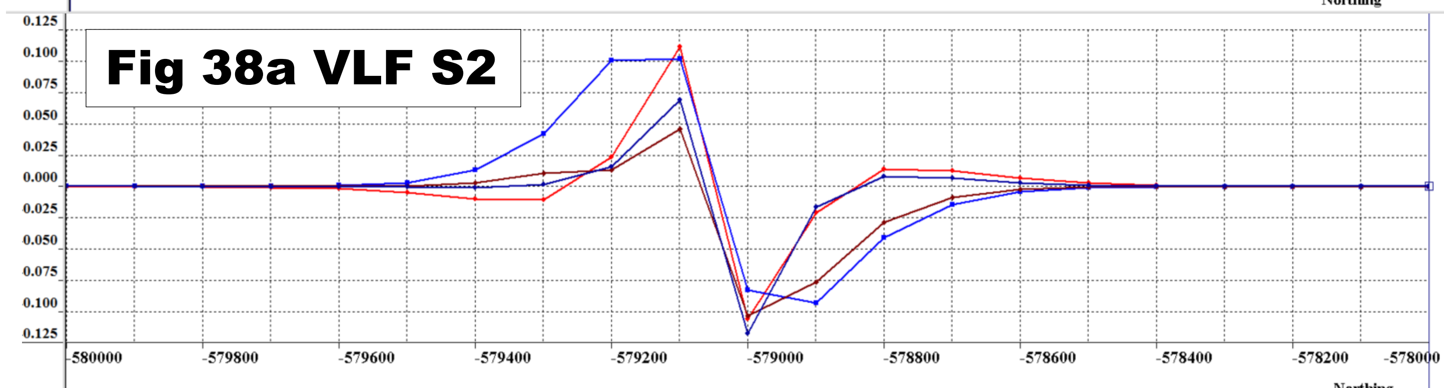

VLF T_x Re S2 | VLF T_x Re S1
VLF T_x Im S2 | VLF T_x Im S1
VLF T_y Re S2 | VLF T_y Re S1
VLF T_y Im S2 | VLF T_y Im S1

Strike – 45NE, Depth to top – 10m, Length – 4km, Width - 25m, Thickness - 800m, Offset from Profile - 0m, Resistivity – 2.5 Ωm , Background – 800 Ωm ,Centre Point NS - -579000

CONCLUSIONS

This study was initiated at the behest of a client to evaluate the benefits of airborne VLF surveys. The study extended out from this to the study of interpretation of both ground and airborne VLF data assuming the data was equivalent to magnetotelluric data and thus MT modeling and inversion software could be utilized to interpret such data. This assumption is quite standard assuming that the vertical electric field has rotated to the horizontal at far distances and that the excitation fields will be in the far field having a 1/r falloff and thus a relatively uniform spatial field. These assumptions are long standing and contained in all the textbooks but we know of no in depth study of these issues.

The fields from the VLF antennae propagate outwards. In our case, we simulate a source radiating independent of the azimuth from the source. The principle components are Ez (φ,r) and Hy(φ,r) and they propagate in the x-direction where x is radial, y is azimuthal and z vertical. The principle components have an asymptotic r^{-2} fall-off in the air. If the air has a resistivity of 10^8 then the wavelength is 12.49km at 24Khz. If there is not a strong ionosphere then there is a slight rotation of Ez to the horizontal even at altitude. The transmitter is simulated as an ungrounded vertical current with its base at ground level

The objective of the study was to demonstrate through simple numerical simulations that the assumptions utilized in developing algorithms for both forward and inverse modeling of magnetotelluric data are not even approximately met by VLF fields no matter how far from the transmitters the data is measured